Published in final edited form as:
J Med Chem. 2009 July 23; 52(14): 4511–4523. doi:10.1021/jm900472s.

Apogossypol Derivatives as Pan-active Inhibitors of Anti-apoptotic B-cell lymphoma/leukemia-2 (Bcl-2) Family Proteins

Jun Wei, **Shinichi Kitada**, **Michele F. Rega**, **John L. Stebbins**, **Dayong Zhai**, **Jason Cellitti**, **Hongbin Yuan**, **Aras Emdadi**, **Russell Dahl**, **Ziming Zhang**, **Li Yang**, **John C. Reed**, and **Maurizio Pellecchia***
Burnham Institute for Medical Research, 10901 North Torrey Pines Rd, La Jolla, CA, 92037, USA.;

Abstract

Guided by nuclear magnetic resonance (NMR) binding assays and computational docking studies, a series of 5, 5′ substituted Apogossypol derivatives was synthesized that resulted in potent pan-active inhibitors of anti-apoptotic Bcl-2 family proteins. Compound 8r inhibits the binding of BH3 peptides to Bcl-X_L, Bcl-2, Mcl-1 and Bfl-1 with IC_{50} values of 0.76, 0.32, 0.28 and 0.73 μM, respectively. The compound also potently inhibits cell growth of human lung cancer and BP3 human B-cell lymphoma cell lines with EC_{50} values of 0.33 and 0.66 μM, respectively. Compound 8r shows little cytotoxicity against *bax*$^{-/-}$*bak*$^{-/-}$ cells, indicating that it kills cancers cells via the intented mechanism. The compound also displays *in vivo* efficacy in transgenic mice in which Bcl-2 is overexpressed in splenic B-cells. Together with its improved chemical, plasma and microsomal stability relative to compound 2 (Apogossypol), compound 8r represents a promising drug lead for the development of novel apoptosis-based therapies for cancer.

Introduction

Programmed cell-death (apoptosis) plays critical roles in the maintenance of normal tissue homeostasis, ensuring a proper balance of cell production and cell loss.[1, 2] Defects in the regulation of programmed cell death promote tumorgenesis, and also contribute significantly to chemoresistance.[3, 4] B-cell lymphoma/leukemia-2 (Bcl-2) family proteins are central regulators of apoptosis.[5–7] In humans, six anti-apoptotic members of the Bcl-2 family have been identified and characterized thus far, including Bcl-2, Bcl-X_L, Mcl-1, Bfl-1, Bcl-W and Bcl-B. Over-expression of anti-apoptotic Bcl-2 family proteins occurs in many human cancers and leukemias, and therefore these proteins are very attractive targets for the development of novel anticancer agents.[8–11] Members of the Bcl-2 family proteins also include pro-apoptotic effectors such as Bak, Bax, Bad, Bim and Bid. Anti-apoptotic and pro-apoptotic Bcl-2 family proteins dimerize and negate each other's functions.[3] Structural studies revealed the presence of a deep and relatively large hydrophobic crevice on the surface of anti-apoptotic Bcl-2 family proteins that binds the BH3 dimerization domain (an α-helical region) of pro-apoptotic family members.[10] Thus, molecules that mimic the BH3 domain of pro-apoptotic proteins induce apoptosis and/or abrogate the ability of anti-apoptotic Bcl-2 proteins to inhibit cancer cell death.

We and others have reported that the natural product **1** (Gossypol) (Figure 1A) is a potent inhibitor of Bcl-2, Bcl-X_L and Mcl-1, functioning as a BH3 mimetic.[12–17] Compound **1** is

*Corresponding author: mpellecchia@burnham.org, Phone: (858) 6463159, Fax: (858) 7955225.

Supporting Information Available: An experimental section including information on the chemical data for compounds (**7a-7t** and **11a-11c**), NMR experiments, isothermal titration calorimetry assays, *in vitro* ADME studies and *in vivo* MTD mice studies. This material is available free of charge via the internet at http://pubs.acs.org.

currently in phase II clinical trials, displaying single-agent antitumor activity in patients with advanced malignancies.[14, 17, 18] In mice studies, compound **1** displays some toxicity and off target effects likely due to two reactive aldehyde groups, which are important for targeting other cellular proteins such as dehydrogenases, for example. Our previous molecular docking studies, however, suggested that these two reactive groups are not essential for the compound to bind to Bcl-2 proteins, hence we designed compound **2** (Apogossypol) (Figure 1A), that lacks the aldehydes. In agreement with our predicted docked structure, compound **2** retains activity against anti-apoptotic Bcl-2 family proteins *in vitro* and in cells.[19] Recently, we further compared the efficacy and toxicity in mice of compounds **1** and **2**. Our preclinical *in vivo* data show that compound **2** has superior efficacy and markedly reduced toxicity compared to **1**.[20] We also evaluated the single-dose pharmacokinetic characteristics of compound **2** in mice. Compound **2** displayed superior blood concentrations over time compared to compound **1**, due to slower clearance.[21] These observations indicate that compound **2** is a promising lead compound for cancer therapy.

Recently, we reported the separation and characterization of atropoisomers of compound **2**.[22] These studies revealed that the racemic compound **2** is as effective as its individual isomers.[22] We further reported the synthesis and evaluation of 5, 5′ ketone substituted compound **2** derivatives. Among these derivatives, compound **3** (BI79D10)[23] displayed improved *in vitro* and *in vivo* efficacy compared to compound **2** (Figure 1A and 1B). However, contrary to what we observed with compound **2**, compound **3** displayed also mild GI toxicity in mice. The observed toxicity in compound **3** may be attributable to relatively active ketone groups.[23] Based on these premises, in this current work, we focused our attention on preparing and evaluating activities of novel 5, 5′ substituted compound **2** derivatives which further replace the reactive ketone groups with more druggable amide and alkyl groups (Figure 1B).

Results and Discussion

We have recently reported that compound **2** is a promising inhibitor of Bcl-X_L and Bcl-2 with improved *in vivo* efficacy and reduced toxicity compared to compound **1**.[12, 19, 20] Molecular docking studies of compound **2** into the BH3 binding groove in Bcl-2 [24, 25] (Figure 1C) suggest that **2** forms two hydrogen bonds with residues Arg 143 and Tyr 105 in Bcl-2 through the 1 and 1′ hydroxyl groups, respectively. Compound **2** is also involved in hydrogen bonding interactions with Trp 141 and Tyr 199 in Bcl-2 through the 6′ hydroxyl group on naphthalene ring. According to this model, the isopropyl group on the left naphthalene ring inserts into the first hydrophobic pocket (P1) in Bcl-2 (Figure 1C), while the isopropyl group on the right naphthalene ring inserts into the second hydrophobic pocket (P2) (Figure 1C). Hence, the analysis of the predicted binding models indicates that while the overall core structure of compound **2** fits rather well into BH3 binding groove of Bcl-2, the two isopropyl groups do not apparently fully occupy the hydrophobic pockets P1 and P2. Therefore, a library of 5, 5′ substituted compound **2** derivatives (Figure 1B) that replace the isopropyl groups with suitable substituents was designed with the aim of deriving novel molecules that could occupy the hydrophobic pockets on Bcl-2 more efficiently.

A synthetic route (Scheme 1) was developed to introduce a variety of amide derivatives at the 5, 5′ positions. Compound **1** was treated with NaOH solution at 90°C to provide compound **2**, which was readily methylated by dimethyl sulfate in the presence of potassium carbonate to afford compound **4**.[26] Reaction of compound **4** with $TiCl_4$ followed by dichloromethyl methyl ether at room temperature resulted in loss of the isopropyl groups and simultaneous bisformylation to give the aldehyde compound **5**.[26] The aldehyde groups of compound **5** were converted to carboxylic acid **6** by mild oxidation with sodium hypochlorite.[27] The carboxylic acid **6** was then coupled with a variety of commercially available amines in the presence of 1-ethyl-3-(3′-dimethylaminopropyl)carbodiimide (EDCI) at room temperature to give

compound **7**.[28] Subsequent demethylation of the compound **7** using boron tribromide afforded compound **8**.[27] The synthesis of 5, 5′ alkyl substituted compound **2** derivatives was outlined in Scheme 2. Compound **5** was treated with different Grignard or lithium reagents to afford a secondary alcohol **9**, which was oxidized to give the phenone **10** by pyridinium chlorochromate. Triethylsilane reduced phenone **10** to alkyl compound **11**[29] followed by subsequent demethylation using boron tribromide to afford compound **12** (Scheme 2). Compounds **13** and **14** (Scheme 3), with only hydrogen atom or carboxylic acid at 5, 5′ positions, were synthesized to explore if substitution at 5, 5′ position is important for enhancing biological activities. Compound **13** was synthesized by treating compound **4** with concentrated sulfuric acid to lose isopropyl group.[26] The resulting product and compound **6** was then treated individually with boron tribromide to give compounds **13** and **14**, respectively (Scheme 3).

The synthesized 5, 5′ substituted compound **2** derivatives were first screened by one-dimensional ^{1}H nuclear magnetic resonance spectroscopy (1D-^{1}H NMR) binding assays against Bcl-X_L, as we reported previously (Table 1 and 2).[30] Active compounds in 1D-^{1}H NMR binding assays were then selected and evaluated in Isothermal Titration Calorimetry assays (ITC), competitive fluorescence polarization assays (FPA) and cell viability assays (Tables 1–3). A group of compounds (**8r**, **8q**, **8m**) displayed high binding affinity to Bcl-X_L in these assays (Table 1, 8r Figure 2A). The most potent compound induced significant chemical shift changes in active site methyl groups (region between −0.38 and 0.42 ppm) in the one-dimensional ^{1}H-NMR spectra of Bcl-X_L (Figure 2A) and also has an IC_{50} value of 0.76 μM in the FP displacement assays, which is 5 times more effective than **2** (Table 3 and Supplementary Figure 2A). To further confirm the results obtained by the NMR binding data and the FP assays, we further evaluated the binding affinity of compound **8r** for Bcl-X_L using ITC assay (Table 3 and Supplementary Figure 1). In agreement with NMR binding and FPA data, compound **8r** displayed potent binding affinity to Bcl-X_L with a K_d value of 0.11 μM, which is 15 times more potent than compound **2** (K_d = 1.7 μM) in the same assay. Consistent with NMR binding, FPA, and ITC data, compound **8r** displayed efficacy in inhibiting growth of PC3ML cells, which express high levels of Bcl-X_L. The EC_{50} value of **8r** is 1.7 μM, hence 6-fold more potent than **2** (EC_{50} = 10.4 μM). Compounds (**8j-8k** and **8p-8s**) displayed similar binding affinity as **8r** for Bcl-X_L in these assays with average IC_{50} value of 2.8 μM (Table 1).

In addition to Bcl-X_L, other members of the Bcl-2 family are known to play critical roles in tumor cell survival.[31, 32] Therefore, we further evaluated the binding properties and specificity of selected 5, 5′ substituted compound **2** derivatives against Bcl-2, Mcl-1 and Bfl-1 using FP assays (Table 3 and Figure 2B). In these assays, compound **8r** inhibited Bcl-2, Mcl-1 and Bfl-1 with IC_{50} values of 0.32, 0.28 and 0.73 μM, respectively, values that correspond to approximately 10 times higher potency thanwhat observed with compound **2** in similar FP assays (Figure 2B, Table 3 and Supplementary Figure 2A). Compound **8r** was further evaluated against H460, H1299 and BP3 cell lines, which express high levels of Bcl-2, Mcl-1 and Bfl-1, respectively (Table 1).[32–34] Consistent with FPA data, compound **8r** displayed significant efficacy in inhibiting growth of H460 and BP3 cells, with IC_{50} values of 0.33 μM and 0.66 μM, repectively, which are approximately 7–10 times more potent than what observed with compound **2** against the same cell lines (Table 1, 8r Figure 2C and Supplementary Figure 3A). Molecular docking studies with compound and Bcl-2 (Figure 1D) suggest that 2-phenylpropyl groups at 5, 5′ positions could insert deeper into hydrophobic pockets (P1 and P2) in Bcl-2, hence occupying these regions more efficiently compared to the isopropyl groups of compound 2 (Figure 1B). In addition, the carbonyl group on the right naphthalene ring also formed an additional hydrogen bond with residue Tyr199. Other 5, 5′ substituted derivatives, such as compounds **12e**, **8n**, **8p**, **8q**, **8k** also displayed strong pan-active inhibitory properties against Bcl-2, Mcl-1 and Bfl-1. The most potent derivative, compound **8q**, inhibits Bcl-2, Mcl-1 and Bfl-1 with IC_{50} values of 0.67, 0.59 and 1.3 μM (Figure 2B and Table 3), respectively, in FP assays. In agreement with these data, the compound showed potent cell growth inhibitory

activity against H460, H1299 and BP3 cell lines, with IC_{50} values of 0.40, 0.36 and 0.20 μM, respectively (Table 1, Figure 2C and Supplementary Figure 3A).

As anticipated by our initial docking studies with compound **2**, the synthesized derivatives reveals that substitution at 5, 5′ position with larger hydrophobic groups result in improved binding affinity to the anti-apoptotic Bcl-2 family proteins tested. Consisted to these observations, compounds **13** and **14** (Table 1 and 2), with only hydrogen atoms or carboxylic acid groups on 5, 5′ positions, displayed weak or no inhibition in all reported in vitro and cellular assays (Table 1 and 2). A closer look at the emerging SAR for the synthesized 5, 5′ amide substituted derivatives further indicates that longer and flexible hydrophobic groups display higher potency than small, short and rigid hydrophobic groups. Replacement of the methylcyclopropane (**8l**) or the cyclopentyl (**8b**) groups by the longer methylcyclohexyl group (**8m**) significantly increased cell inhibition potency. Also, compounds (**8n-8s**) having phenethyl groups at 5, 5′ positions displayed potent cell activity in the H460 and PC3ML cell lines with average EC_{50} values of 0.64 μM and 2.6 μM, respectively, while related compounds (**8a-8e**) having only phenyl groups displayed relatively weaker cell activity with average EC_{50} values of 8.6 μM and 11.3 μM, respectively (Table 1) against the same cell lines.

These observations are corroborated by our computational docking studies suggesting that longer and flexible groups may insert deeper into the P1 and P2 pockets (Figure 1C and 1D).

We further explored the SAR of the 5, 5′ alkyl substituted derivatives. Overall we observed the similar trend that suggests longer, hydrophobic groups to improve potency. Compounds **12a** and **12b** with isobutyl and isopentyl groups displayed improved activity compared to **2** with isopropyl groups. Similarly, compound **12e** with phenethyl groups is more active than compound **12d** with benzyl groups (Table 2).

Next, we profiled the activity of the compounds in cells and compared their cell killing ability with their reported levels of Bcl-2 proteins. For example, the lung cancer H460 cell line has been studied by several groups with respect to sensitivity to Bcl-2 antagonists.[33–35] In our studies, however, we also introduce the BP3 cell line to profile compounds' activity. The BP3 cell line originates from a human diffuse large B-cell lymphoma (DLBCL) overexpressing Bfl-1. The mRNA ratio of Bfl-1, Bcl-X_L and Mcl-1 is approximately 10:3:1.[32] However, we determined that BP3 cells express high levels of both Bfl-1 and Mcl-1 by Western blot analysis (Supplementary Table 1). In agreement with these observations, the potent dual Bcl-X_L and Bcl-2 antagonist, compound **15** (ABT-737) 24 displayed no cytotoxic activity against BP3 cell lines presumably because this molecule is not effective against Mcl-1 and Bfl-1 (Supplementary Figure 2B).[24, 31, 36] By comparison, our most active compounds **8q** and **8r**, targeting Bfl-1 and Mcl-1, showed submicromolar cell growth inhibitory activity against BP3 cells with IC_{50} values of 0.20 and 0.66 μM, respectively (Table 1). We also evaluated the ability of 5, 5′ derivatives to induce apoptosis of the human lymphoma RS11846 cell line, which expresses high levels of Bcl-2 and Bcl-X_L. For these assays, we used Annexin V-FITC and propidium iodide (PI) double staining, followed by flow-cytometry analysis (Table 1). Most of synthesized derivatives effectively induced apoptosis of the RS11846 cells in a dose-dependent manner (Table 1 and Supplementary Figure 3B). In particular, compounds **8q**, **8r** and **8n** are effective with EC_{50} values ranging from 3.0 to 5.8 μM, which is consistent with previous results obtained for human PC3ML and H460 cancer cell lines. Again, the negative control compounds **13** and **14** induced little or no apoptosis of the RS11846 cell line.

We next explored whether 5, 5′ substituted compound **2** derivatives had cytotoxicity against wild type mouse embryonic fibroblast cells (wt-MEFs) and transformed Bax/Bak double knockout MEF cells (DKO/MEFs) in which anti-apoptotic Bcl-2 family proteins lack a cytoprotective phenotype.[37, 38] The most potent pan-active Bcl-2 compound **2** derivatives,

namely compounds **8m**, **8q**, **8r**, **8k**, **8p**, induced nearly complete cell death (80–90%) of wt-MEFs at 10 μM (Figure 2D). However, at the same concentration they are ineffective in killing DKO/MEFs measured by the same FITC-Annexin V/PI assay (Figure 2D). These data strongly suggest that cytotoxic activities of those compound **2** derivatives are largely dependant on the Bcl-2 pathway. In contrast, compound **1** seems equally effective in killing both wt MEFs and MEF/DKOs at 10 μM (Figure 2D), suggesting that other possible killing mechanisms not related to Bcl-2 inhibition are induced by this compound. Due to the lack of the reactive aldehydes of compound **1**, compound **2** showed improved selectivity against Bcl-2 proteins hence reduced cytotoxicity against MEF/DKOs (Figure 2D). Recently, Vogler *et al*.[38] based on an extensive sets of validation studies on a panel of reported Bcl-2 antagonists, including compounds **1** and **2**, concluded that only the Abbott compound ABT-737 shows remarkable selectivity for Bcl-2 and Bcl-xL. However, among the compounds examined, Vogler *et al*. also concluded that it is possible that analogs of compounds **1** and **2** may have the potential for becoming selective Bcl-2 antagonists.[38] This conclusion is now corroborated by our studies that resulted in more potent pan-active Bcl-2 antagonists.

Compound **2** is a polyphenol scaffold with six hydroxyl groups on the naphthalene ring (Figure 1A) which can be oxidized to quinones. We previously stabilized **2** by co-crystalizing it with ascorbic acid.[22] Compound **2** can also be stabilized by introducing electron withdrawing groups, such as carbonyl groups on the naphthalene rings, which slow oxidation and other side reactions. The chemical stability of our compounds (**8m**, **8q**, **8r**, **8k**, **8p**, **12e**) was evaluated as solid powders at room temperature. Compound stability was monitored using a combination of HPLC and LC-MS. Overall, 5, 5′ amide substituted compound **2** derivatives show superior chemical stability compared to **2** (Figure 3A). In particular, **8r** and **8q** were only 10% degraded after 60 days at room temperature while **2** is almost 80% decomposed under the same condition in the absence of ascorbic acid. Compound **12e** having phenethyl groups at the 5, 5′ positions are also less stable than amide compounds, presumably due to the lack of electron withdrawing groups.

To test the pharmacological properties of 5, 5′ substituted compound **2** derivatives, we determined their *in vitro* plasma stability, microsomal stability, and cell membrane permeability (Table 4). From these studies, we could conclude that our synthesized compounds displayed superior plasma and microsomal stability compared to **2** (Table 4). Compounds **8r** and **8m** only degraded 4% and 11%, respectively, after 1 h incubation in rat plasma while **2** degraded 47% under the same conditions. In addition, compounds **8r** and **8m** degraded by 24% and 10%, respectively, after 1 h incubation in rat microsomal preparations, while **2** degraded by 36% under the same conditions (Table 4). Compounds **8r** and **8m** also showed similar or improved cell membrane permeability compared to **2**.

Hence, using a combination of NMR-based binding assays, FP assays, ITC assays, cytotoxicity assays and preliminary *in vitro* ADME data, we selected compounds to be tested in subsequent *in vivo* studies using a Bcl-2 transgenic mouse model. B-cells of the B6 transgenic mice overexpress human Bcl-2 and accumulate in the spleen of mice. The spleen weight is used as an end-point for assessing *in vivo* activity as we have determined that the spleen weight is highly consistent in age- and sex-matched Bcl-2-transgenic mice, varying by only ±2% among control Bcl2 mice.[20] We first screened the *in vivo* activities of compounds such as **8r** and **8q** side by side with **1** and **2** in Bcl-2 transgenic mice with a single intraperitoneal (ip) injection at 72 μmol/kg. In agreement with the *in vitro* data, tested 5, 5′ amide substituted compound **2** derivatives displayed superior *in vivo* activity compared to **1** and **2** (Figure 3B). In particular, compounds (**8r**, **8k** and **8p**) induced more than 40% spleen weight reduction compared to only ≤20% by **1** and **2**. Since the maximum spleen shrinkage would be no more than 50% in this experimental model,[20] these compounds induced near maximal (85–95%) biological activity, while **1** and **2** induced ≤40% of maximum reduction in spleen weight at the same dose. The

negative control, compound **13**, displayed no activity in transgenic mice, as expected. Overall, the 5, 5′ alkyl substituted compound **2** derivatives tested (**12c** and **12e**) displayed lower *in vivo* activity compared to 5, 5′ amide substituted compound **2** derivatives. However, the 5, 5′ alkyl substituted compound **2** derivatives show no significant signs of toxicity at 72 μmol/kg and even at 120 μmol/kg while 5, 5′ amide substituted compound **2** derivatives show evidence of toxicity at the 72 μmol/kg (Supplementary Table 2). In particular, mice treated with compound **8r** had more apparent signs of GI toxicity at the 72 μmol/kg dose (50 mg/kg).

To balance the toxicity verse efficacy of compound **8r**, we next explored the maximum tolerated dose (MTD) of **8r** using a group of five mice. Mice were treated with a single dose of 100, 75, 50 and 25 mg/kg (ip) and observed for a period of 14 days monitoring morbidity (body weight loss) and mortality. All mice were alive after 14 days. The maximum weight loss was observed at the fifth day, with 80–100% recovery after 14 days (Figure 3C). The mice dosed at 25 mg/kg showed slightly weight loss, while the mice dosed at 50 mg/kg displayed <15% weight loss. Therefore the MTD of compound **8r** is likely between 25 mg to 50 mg/kg. We next evaluated the *in vivo* activity and toxicity of the compound **8r** in groups of six mice each at a dose of 42 mg/kg (60 μmol/kg). Consistent with the single mouse experiment, compound **8r** treatment resulted in a significant (~70%) reduction of spleen weight ($P<0.0001$) compared to the control group of six mice (Figure 3D). All mice tolerated the treatment well, with only mild signs of GI toxicity. The average weight loss of mice was 7.8% during the course of this study of compound **8r**.

Conclusions

In summary, a library of 5, 5′ substituted compound **2** derivatives was synthesized and evaluated in a variety of *in vitro* and *in vivo* assays. The most potent compound, **8r**, was found to bind to Bcl-x_L, Bcl-2, Mcl-1 and Bfl-1 with IC_{50} values of 760 nM, 320 nM, 280 nM and 730 nM, respectively. The compound also potently inhibited growth in cultures of the PC3ML, H460, H1299 and BP3 cancer cell lines, which express Bcl-X_L, Bcl-2, Mcl-1 and Bfl-1, respectively, with EC_{50} values in the submicromolar to nanomolar range. Compound **8r** effectively induced apoptosis of the RS11846 human lymphoma cell line in a dose-dependent manner and show little cytotoxicity against Bax/Bak double knockout mouse embryonic fibroblast cells in which anti-apoptotic Bcl-2 family proteins lack a cytoprotective phenotype. Hence, compound **8r** is much more effective against Bcl-2 proteins in *in vitro* assays resulting in increased cytotoxicity against cancer cells compared to compounds **1** and **2**, and descreased cytotoxicity against Bax/Bak MEF/DKO cells, suggesting that owe to its increased affinity for the Bc-2 proteins, off target effects that characterize cell death induced by compounds **1** and **2**, respectively, are much less prominent in this compound. Finally, compound **8r** showed favorable chemical stability, *in vitro* ADME properties, and superior *in vivo* efficacy compared to **2** in Bcl-2 transgenic mice in which Bcl-2 is overexpressed in B-cells. Considering the critical roles of anti-apoptotic Bcl-2 family proteins in tumorgenesis and chemoresistance, and the potent inhibitory activity of **8r** against anti-apoptotic Bcl-2 family proteins, we speculate that this compound represents a viable drug candidate for the development of novel apoptosis-based cancer therapies.

Experimental Section

General Synthetic Procedures

Unless otherwise indicated, all reagents and anhydrous solvents (CH_2Cl_2, THF, diethyl ether, etc) were obtained from commercial sources and used without purification. All reactions were performed in oven-dried glassware. All reactions involving air or moisture sensitive reagents were performed under a nitrogen atmosphere. Silica gel or reverse phase chromatography was performed using prepacked silica gel or C-18 cartridges (RediSep), repectively. All final

compounds were purified to > 95% purity, as determined by a HPLC Breeze from Waters Co. using an Atlantis T3 3 μM 4.6 mm × 150 mm reverse phase column. Compounds for *in vivo* studies were purified to ≥ 98% purity using preparative HPLC. The eluant was a linear gradient with a flow rate of 1 mL/min from 50% A and 50% B to 5% A and 95% B in 15 min followed by 5 min at 100% B (Solvent A: H_2O with 0.1% TFA; Solvent B: ACN with 0.1% TFA). Compounds were detected at λ = 254 nm. ^{1}H NMR spectra were recorded on Varian 300 or Bruker 600 MHz instruments. Chemical shifts are reported in ppm (d) relative to ^{1}H (Me_4Si at 0.00 ppm). Coupling constant (*J*) are reported in Hz throughout. Mass spectral data were acquired on Shimadzu LCMS-2010EV for low resolution, and on an Agilent ESI-TOF for high resolution.

1,1′,6,6′,7,7′-Hexahydroxy-5,5′-diisopropyl-3,3′-dimethyl-2,2′-binaphthyl-8,8′-dicarboxaldehyde (1)—Compound **1** is commercially available from Yixin Pharmaceutical Co. HPLC purity 99.0%, t_R = 12.50 min.

5,5′-Diisopropyl-1,1′,6,6′,7,7′-hexahydroxy-3,3′-dimethyl-2,2′-binaphthalene (2)—The compound **1** (5 g, 8.65 mmol) in 50 mL of 40% NaOH was heated under nitrogen at 90 °C for 3.5 h in the dark. The reaction mixture was cooled and poured slowly onto ice (300 mL) and concentrated H_2SO_4 (35 mL) mixture to form white precipitation. The precipitation was filtered, washed with water and dried to afford 3.8 g of compound **2** (95%) as a white solid. ^{1}H NMR (300 MHz, $CDCl_3$) δ 7.61 (s, 2H), 7.50 (s, 2H), 5.93 (s, 2H), 5.27 (s, 2H), 5.13 (s, 2H), 3.88 (m, 2H), 2.12 (s, 6H), 1.55 (d, *J* = 5.5 Hz, 12H). HPLC purity 99.2%, t_R = 13.12 min. HRMS calcd for $\mathbf{C_{28}H_{30}O_6}$ 463.2115 (M + H), found 463.2108.

5,5′-Diisopropyl-1,1′,6,6′,7,7′-hexamethoxy-3,3′-dimethyl-2,2′-binaphthalene (4)—The compound **2** (3.8 g, 8.21 mmol) was dissolved into acetone (200 mL). K_2CO_3 (23.9 g, 206.7 mmol) and dimethyl sulfate (16.3 mL, 206.7 mmol) were added and the reaction mixture was refluxed under nitrogen for 24 h. The solid was collected by filtration and washed using acetone and water and dried to yield 4.2 g of compound **4** as white solid (93%). ^{1}H NMR (300 MHz, $CDCl_3$) 7.83 (s, 2H), 7.43 (s, 2H), 3.98 (m, 8H), 3.94 (s, 6H), 3.57 (s, 6H), 2.20 (s, 6H), 1.56 (s, 12H).

1,1′,6,6′,7,7′-Hexamethoxy-3,3′-dimethyl-2,2′-binaphthalene-5,5′-dicarboxaldehyde (5)—To a solution of compound **4** (1.6 g, 2.93 mmol) in dry methylene chloride (40 mL) at 0 °C was added titanium tetrachloride (14.3 g, 75.5 mmol). After addition was completed, the dark red solution was stirred an additional 15 min at 0 °C. Dichloromethyl methyl ether (2.93 g, 25.5 mmol) was added dropwise over 15 min, and the reaction mixture was stirred at ambient temperature under nitrogen for 12 h. The reaction mixture was poured onto ice and the resulting aqueous layer was extracted twice with methylene chloride. The combined organic fractions were washed with water and brine, dried over $MgSO_4$, and concentrated to give dark red oil. The oil was chromatographed (acetonitrile/methylene chloride) followed by trituration of crude product with diethyl ether to afford compound **5** (0.60 g, 40%) as yellow solid. ^{1}H NMR (300 MHz, $CDCl_3$) 10.84 (s, 2H), 8.93 (s, 2H), 7.82 (s, 2H), 4.10 (s, 6H), 4.03 (s, 6H), 3.48 (s, 6H), 2.22 (s, 6H).

1,1′,6,6′,7,7′-Hexamethoxy-3,3′-dimethyl-2,2′-binaphthalene-5,5′-dicarboxylic acid (6)—Compound **5** (6.6 g, 12.7 mmol) was dissolved in 40 mL of acetonitrile and 40 mL of THF in an ice bath. Sodium dihydrogen phosphate (876 mg, 6.35 mmol), 30% hydrogen peroxide (2.6 mL, 25.4 mmol) were added. Sodium chlorite (4.14 g, 45.8 mmol) dissolved in 20 mL of water was added. The reaction mixture was stirred overnight at room temperature and then poured onto 100 g of ice with 30 mL of 6M HCl. The solution was extracted with ether (3 × 100 mL). The ether extracts were washed with brine, dried over magnesium sulfate

and filtered. Evaporation of the solvent *in vacuo* and the residue was purified by C-18 column chromatography (H_2O/Acetonitrile) to give 5.9 g (85%) of compound **6** as a red solid. ^{1}H NMR (600 MHz, CD_3OD) δ 8.0 (s, 2H), 7.68 (s, 2H), 4.1 (s, 6H), 4.06 (s, 6H), 3.54 (s, 6H), 2.21 (s, 6H).

1,1′,6,6′,7,7′-Hexamethoxy-3,3′-dimethyl-N^5,N$^{5'}$-bis(2-phenylpropyl)-2,2′-binaphthyl-5,5′-dicarboxamide (7r)—Compound **6** (500 mg, 0.907 mmol), EDCI (522 mg, 2.72 mmol) and HOBT (244 mg, 1.81 mmol) were dissolved in 15 mL of dry CH_2Cl_2 and stirred at room temperature for 10 min under nitrogen atmosphere. 2-phenyl-1-propanamine (0.30 mL, 2.09 mmol) and Et_3N (0.51 mL, 3.7 mmol) were added and the reaction mixture was stirred at room temperature for 24 h. The mixture was then poured onto 50 mL of water and the solution was extracted with CH_2Cl_2 (3 × 100 mL). The ether extracts were washed with water and brine, dried over magnesium sulfate and filtered. Evaporation of the solvent *in vacuo* and the residue was purified by silica chromatography to give 320 mg (45%) of compound **7r** as a yellow solid. ^{1}H NMR (600 MHz, CD_3OD) δ 7.56 (s, 2H), 7.37 (m, 8H), 7.22 (m, 4H), 3.98 (s, 6H), 3.85 (s, 6H), 3.77 (m, 2H), 3.62 (m, 2H), 3.55 (s, 3H), 3.53 (s, 3H), 3.20 (m, 2H), 2.01 (s, 3H), 2.00 (s, 3H), 1.38 (s, 3H), 1.39 (s, 3H).

1,1′,6,6′,7,7′-Hexahydroxy-3,3′-dimethyl-N^5,N$^{5'}$-bis(2-phenylpropyl)-2,2′-binaphthyl-5,5′-dicarboxamide (8r)—0.45 mL of BBr_3 solution (1.18 g, 4.73 mmol) was added dropwise into a solution of compound **7** (310 mg, 0.40 mmol) in 20 mL of anhydrous CH_2Cl_2 at −78 °C. Stirring was continued at −78 °C for 1 h, 0 °C for 1 h, and ambient temperature for 1 h. 50 grams of ice containing 10 mL of 6M HCl was added to the mixture and stirred for 1 h at room temperature. The aqueous layer was extracted with dichloromethane (3 × 50 mL). The combined organic layer was washed with water, brine and dried over $MgSO_4$. The solvent was concentrated *in vacuo* and the residue was purified using C-18 column chromatography (H_2O/Acetonitrile) to give 200 mg of compound **8r** (72%) as white-yellow solid. ^{1}H NMR (600 MHz, CD_3OD) δ 7.56 (s, 2H), 7.37 (d, J = 6.0 Hz, 4H), 7.32 (t, $J_1 = J_2$ = 7.2 Hz, 4H), 7.20 (t, $J_1 = J_2$ = 7.2 Hz, 2H), 7.07 (s, 1H), 6.99 (s, 1H), 3.76-3.60 (m, 4H), 3.19 (m, 2H), 1.90 (d, J = 3.0 Hz, 3H), 1.88 (d, J = 3.0 Hz, 3H), 1.41 (m, 6H); HPLC purity 99.4%, t_R = 8.71 min. HRMS calcd for **$C_{42}H_{40}N_2O_8$** 701.2857 (M + H), found 701.2864.

Following above mentioned procedure and the appropriate starting materials and reagents used; compounds **8a-8t** were synthesized.

1,1′,6,6′,7,7′-Hexahydroxy-3,3′-dimethylN^5,N$^{5'}$-diphenyl-2,2′-binaphthyl-5,5′-dicarboxamide (8a)—Yield, 75%; ^{1}H NMR (600 MHz, CD_3OD) δ 7.77 (d, J = 7.8 Hz, 4H), 7.63 (s, 2H), 7.38 (t, J_1 = 7.8 Hz, J_2 = 7.2 Hz, 4H), 7.28 (s, 2H), 7.16 (t, J_1 = 7.8 Hz, J_2 = 7.2 Hz, 2H), 2.01 (s, 6H). HPLC purity 98.0%, t_R = 5.95 min. HRMS calcd for **$C_{36}H_{28}N_2O_8$** 617.1918 (M + H), found 617.1912.

N^5,N$^{5'}$-Dicyclopentyl-1,1′,6,6′,7,7′-hexahydroxy-3,3′-dimethyl-2,2′-binaphthyl-5,5′-dicarboxamide (8b)—Yield, 76%; ^{1}H NMR (600 MHz, CD_3OD) δ 7.57 (s, 2H), 7.19 (s, 2H), 4.46 (m, 2H), 2.09 (m, 4H), 1.97 (s, 6H), 1.80 (m, 4H), 1.69 (m, 8H). HPLC purity 98.1%, t_R = 4.23 min. HRMS calcd for **$C_{34}H_{36}N_2O_8$** 601.2544 (M + H), found 601.2531.

1,1′,6,6′,7,7′-Hexahydroxy-3,3′-dimethylN^5,N$^{5'}$-bis(4-phenoxyphenyl)-2,2′-binaphthyl-5,5′-dicarboxamide (8c)—Yield, 65%; ^{1}H NMR (600 MHz, CD_3OD) δ 7.78 (d, J = 8.4 Hz, 4H), 7.64 (s, 2H), 7.35 (t, J_1 = 7.8 Hz, J_2 = 7.8 Hz, 4H), 7.28 (s, 2H), 7.08 (m, 2H), 7.02 (m, 8H), 2.01 (s, 6H). HPLC purity 99.0%, t_R = 12.09 min. HRMS calcd for **$C_{48}H_{36}N_2O_{10}$** 801.2443 (M + H), found 801.2425.

N^5,$N^{5\prime}$-Bis(3-ethylphenyl)-1,1′,6,6′,7,7′-hexahydroxy-3,3′-dimethyl-2,2′-binaphthyl-5,5′-dicarboxamide (8d)—Yield, 69%; ^{1}H NMR (600 MHz, CD_3OD) δ7.63 (s, 4H), 7.60 (d, J = 7.8 Hz, 2H), 7.28 (m, 4H), 7.02 (d, J = 7.8 Hz, 2H), 2.68 (q, $J_1 = J_2$ = 8.4 Hz, 4H), 2.01 (s, 6H), 1.28 (t, $J_1 = J_2$ = 8.4 Hz, 6H). HPLC purity 99.5%, t_R = 10.27 min. HRMS calcd for $\mathbf{C_{40}H_{36}N_2O_8}$ 673.2544 (M + H), found 673.2537.

1,1′,6,6′,7,7′-Hexahydroxy-3,3′-dimethylN^5,$N^{5\prime}$-bis(3-(trifluoromethyl) phenyl)-2,2′-binaphthyl-5,5′-dicarboxamide (8e)—Yield, 69%; ^{1}H NMR (600 MHz, CD_3OD) δ 8.26 (s, 2H), 7.96 (d, J = 7.8 Hz, 2H), 7.65 (s, 2H), 7.57 (t, $J_1 = J_2$ = 6.6 Hz, 2H), 7.44 (d, J = 7.2 Hz, 2H), 7.27 (s, 2H), 2.01 (s, 6H). HPLC purity 99.0%, t_R = 13.52 min. HRMS calcd for $\mathbf{C_{38}H_{26}F_6N_2O_8}$ 751.1511 (M + H), found 751.1506.

1,1′,6,6′,7,7′-Hexahydroxy-3,3′-dimethylN^5,$N^{5\prime}$-bis(1-phenylpropyl)-2,2′-binaphthyl-5,5′-dicarboxamide (8f)—Yield, 70%; ^{1}H NMR (600 MHz, CD_3OD) δ 7.50 (m, 4H), 7.31 (m, 6H), 7.09 (s, 2H), 6.95 (s, 2H), 5.09 (m, 2H), 1.88 (m, 6H), 1.09 (m, 6H). HPLC purity 99.3%, t_R = 8.09 min. HRMS calcd for $\mathbf{C_{40}H_{40}N_2O_8}$ 701.2857 (M + H), found 701.2867.

N^5,$N^{5\prime}$-Dibenzyl-1,1′,6,6′,7,7′-hexahydroxy-3,3′-dimethyl-2,2′-binaphthyl-5,5′-dicarboxamide (8g)—Yield, 78%; ^{1}H NMR (600 MHz, CD_3OD) δ 7.58 (s, 2H), 7.54 (d, J = 7.2 Hz, 4H), 7.36 (t, $J_1 = J_2$ = 7.2 Hz, 4H), 7.27 (t, $J_1 = J_2$ = 7.2 Hz, 2H), 7.16 (s, 2H), 4.70 (s, 4H), 1.91 (s, 6H). HPLC purity 99.0%, t_R = 4.92 min. HRMS calcd for $\mathbf{C_{38}H_{32}N_2O_8}$ 645.2231 (M + H), found 645.2237.

1,1′,6,6′,7,7′-Hexahydroxy-3,3′-dimethylN^5,$N^{5\prime}$-bis(3-methylbenzyl)-2,2′-binaphthyl-5,5′-dicarboxamide (8h)—Yield, 75%; ^{1}H NMR (600 MHz, CD_3OD) δ 7.58 (s, 1H), 7.36 (s, 2H), 7.30 (d, J = 7.8 Hz, 2H), 7.23 (t, J_1 = 7.8 Hz, J_2 = 7.2 Hz, 2H), 7.16 (s, 2H), 7.08 (d, J = 7.2 Hz, 2H), 4.65 (t, $J_1 = J_2$ = 15.0 Hz, 4H), 2.36 (s, 6H), 1.91 (s, 6H). HPLC purity 99.0%, t_R = 6.22 min. HRMS calcd for $\mathbf{C_{40}H_{36}N_2O_8}$ 673.2544 (M + H), found 673.2536.

N^5,$N^{5\prime}$-Bis(3-chlorobenzyl)-1,1′,6,6′,7,7′-hexahydroxy-3,3′-dimethyl-2,2′-binaphthyl-5,5′-dicarboxamide (8i)—Yield, 70%; ^{1}H NMR (600 MHz, CD_3OD) δ 7.59 (d, J = 4.2 Hz, 4H), 7.46 (d, J = 7.2 Hz, 2H), 7.35 (t, $J_1 = J_2$ = 7.2 Hz, 2H), 7.28 (d, J = 7.2 Hz, 2H), 7.15 (s, 2H), 4.68 (s, 4H), 1.93 (s, 6H). HPLC purity 98.0%, t_R = 6.71 min. HRMS calcd for $\mathbf{C_{38}H_{30}N_2O_8}$ 713.1452 (M + H), found 713.1426.

1,1′,6,6′,7,7′-Hexahydroxy-3,3′-dimethylN^5,$N^{5\prime}$-bis(2,4,6-trimethylbenzyl)-2,2′-binaphthyl-5,5′-dicarboxamide (8j)—Yield, 70%; ^{1}H NMR (600 MHz, CD_3OD) δ 7.54 (s, 2H), 7.18 (s, 2H), 6.87 (s, 4H), 4.70 (s, 4H), 2.46 (s, 12H), 2.22 (s, 6H), 1.91 (s, 6H). HPLC purity 98.8%, t_R = 10.45 min. HRMS calcd for $\mathbf{C_{44}H_{44}N_2O_8}$ 729.3170 (M + H), found 729.3167.

N^5,$N^{5\prime}$-Bis(1-(4-chlorophenyl)ethyl)-1,1′,6,6′,7,7′-hexahydroxy-3,3′-dimethyl-2,2′-binaphthyl-5,5′-dicarboxamide (8k)—Yield, 73%; ^{1}H NMR (600 MHz, CD_3OD) δ 7.53 (m, 6H), 7.35 (m, 4H), 7.09 (s, 2H), 6.95 (s, 2H), 5.33 (m, 2H), 1.91 (s, 3H), 1.86 (s, 3H), 1.56 (m, 3H), 1.54 (m, 3H). HPLC purity 99.5%, t_R = 8.73 min. HRMS calcd for $\mathbf{C_{40}H_{34}N_2O_8}$ 741.1765 (M + H), found 741.1763.

N^5,$N^{5\prime}$-Bis(cyclopropylmethyl)-1,1′,6,6′,7,7′-hexahydroxy-3,3′-dimethyl-2,2′-binaphthyl-5,5′-dicarboxamide (8l)—Yield, 70%; ^{1}H NMR (600 MHz, CD_3OD) δ 7.58 (s, 2H), 7.26 (s, 2H), 3.36 (m, 4H), 1.97 (s, 6H), 1.18 (m, 2H), 0.57 (d, J = 8.1 Hz, 4H), 0.37

(m, 4H). HPLC purity 98.5%, t_R = 3.95 min. HRMS calcd for **$C_{32}H_{32}N_2O_8$** 573.2231 (M + H), found 573.2214.

$N^5,N^{5\prime}$-Bis(cyclohexylmethyl)-1,1′,6,6′,7,7′-hexahydroxy-3,3′-dimethyl-2,2′-binaphthyl-5,5′-dicarboxamide (8m)—Yield, 80%; ^{1}H NMR (600 MHz, CD_3OD) δ 7.58 (s, 2H), 7.22 (s, 2H), 3.32 (m, 4H), 1.96 (s, 6H), 1.79 (d, *J* = 7.2 Hz, 4H), 1.71 (d, *J* = 8.4 Hz, 4H), 1.39-1.08 (m, 14H). HPLC purity 99.5%, t_R = 9.24 min. HRMS calcd for **$C_{38}H_{44}N_2O_8$** 657.3170 (M + H), found 657.3169.

1,1′,6,6′,7,7′-Hexahydroxy-3,3′-dimethyl$N^5,N^{5\prime}$-diphenethyl-2,2′-binaphthyl-5,5′-dicarboxamide (8n)—Yield, 80%; ^{1}H NMR (600 MHz, CD_3OD) δ 7.58 (s, 2H), 7.36 (d, *J* = 7.2 Hz, 4H), 7.31 (t, $J_1 = J_2$ = 7.2 Hz, 4H), 7.21 (t, $J_1 = J_2$ = 7.2 Hz, 2H), 7.09 (s, 2H), 3.74 (m, 4H), 3.01 (t, $J_1 = J_2$ = 7.2 Hz, 4H), 1.92 (s, 6H). HPLC purity 99.2%, t_R = 5.89 min. HRMS calcd for **$C_{40}H_{36}N_2O_8$** 673.2544 (M + H), found 673.2536.

1,1′,6,6′,7,7′-Hexahydroxy-3,3′-dimethyl$N^5,N^{5\prime}$-bis(3-methylphenethyl)-2,2′-binaphthyl-5,5′-dicarboxamide (8o)—Yield, 76%; ^{1}H NMR (600 MHz, CD_3OD) δ 7.57 (s, 2H), 7.23 (d, *J* = 7.8 Hz, 4H), 7.11 (d, *J* = 7.8 Hz, 4H), 7.06 (s, 2H), 3.80 (m, 4H), 2.96 (t, $J_1 = J_2$ = 7.2 Hz, 4H), 2.29 (s, 6H), 1.90 (s, 6H), 1.40 (s, 4H). HPLC purity 98.0%, t_R = 7.83 min. HRMS calcd for **$C_{40}H_{40}N_2O_8$** 701.2857 (M + H), found 701.2859.

$N^5,N^{5\prime}$-Bis(3-chlorophenethyl)-1,1′,6,6′,7,7′-hexahydroxy-3,3′-dimethyl-2,2′-binaphthyl-5,5′-dicarboxamide (8p)—Yield, 70%; ^{1}H NMR (600 MHz, CD_3OD) δ 7.57 (s, 2H), 7.39 (s, 2H), 7.30 (t, J_1 = 7.2 Hz, J_2 = 6.6 Hz, 4H), 7.21 (d, *J* = 6.6 Hz, 2H), 7.03 (s, 2H), 3.79 (m, 2H), 3.70 (m, 2H), 3.00 (m, 4H), 1.91(s, 6H). HPLC purity 98.5%, t_R = 7.72 min. HRMS calcd for **$C_{40}H_{34}N_2O_8$** 741.1765 (M + H), found 741.1769.

$N^5,N^{5\prime}$-Bis(4-ethylphenethyl)-1,1′,6,6′,7,7′-hexahydroxy-3,3′-dimethyl-2,2′-binaphthyl-5,5′-dicarboxamide (8q)—Yield, 75%; ^{1}H NMR (600 MHz, CD_3OD) δ 7.58 (s, 2H), 7.26 (d, *J* = 7.8 Hz, 4H), 7.15 (d, *J* = 7.8 Hz, 4H), 7.10 (s, 2H), 3.75 (m, 2H), 3.70 (m, 2H), 2.98 (t, $J_1 = J_2$ = 7.2 Hz, 4H), 2.60 (q, J_1 = 7.8 Hz, J_2 = 7.2 Hz, 4H), 1.91 (s, 6H), 1.20 (t, J_1 = 7.8 Hz, J_2 = 7.2 Hz, 6H). HPLC purity 99.7%, t_R = 11.44 min. HRMS calcd for **$C_{44}H_{44}N_2O_8$** 729.3170 (M + H), found 729.3175.

$N^5,N^{5\prime}$-Bis(2,3-dihydro-1H-inden-2-yl)-1,1′,6,6′,7,7′-hexahydroxy-3,3′-dimethyl-2,2′-binaphthyl-5,5′-dicarboxamide (8s)—Yield, 72%; ^{1}H NMR (600 MHz, CD_3OD) δ 7.57 (s, 2H), 7.24 (s, 4H), 7.19 (s, 2H), 7.14 (s, 4H), 4.94 (m, 2H), 3.42 (m, 4H), 3.07 (m, 4H), 1.94 (s, 6H). HPLC purity 98.5%, t_R = 6.66 min. HRMS calcd for **$C_{42}H_{36}N_2O_8$** 697.2544 (M + H), found 697.2541.

$N^5,N^{5\prime}$-Bis(4-chlorophenethyl)-1,1′,6,6′,7,7′-hexahydroxy-3,3′-dimethyl-2,2′-binaphthyl-5,5′-dicarboxamide (8t)—Yield, 75%; ^{1}H NMR (600 MHz, CD_3OD) δ 7.57 (s, 2H), 7.35 (d, *J* = 7.8 Hz, 4H), 7.30 (d, *J* = 7.8 Hz, 4H), 7.02 (s, 2H), 3.76 (m, 2H), 3.71 (m, 2H), 2.99 (t, $J_1 = J_2$ = 6.6 Hz, 4H), 1.93 (s, 6H). HPLC purity 98.7%, t_R = 8.12 min. HRMS calcd for **$C_{40}H_{34}N_2O_8$** 741.1765 (M + H), found 741.1765.

1,1′,6,6′,7,7′-Hexamethoxy-3,3′-dimethyl-5,5′-diphenethyl-2,2′-binaphthalene (11e)—To a freshly benzylmagnesium chloride (5.4 mmol) solution at room temperature was added a solution of **5** (1.0 g, 1.93 mmol) in anhydrous tetrahydrofuran (15 mL) and the reaction mixture was stirred at this temperature for 12 h. The reaction mixture was poured onto saturated ammonium chloride solution and the aqueous layer was extracted twice with diethyl ether, washed with brine and dried over $MgSO_4$. Filtration followed by evaporation of the ether gave

yellow oil. The solution of yellow oil in dry methylene chloride (10 mL) was added into pyridinium chlorochromate (2.6 g, 12.1 mmol) in dry methylene chloride (12 mL). The reaction mixture was stirred at ambient temperature for 4 h and was filtrated through celite. The filtrate was chromatographed to afford 0.3 g of **10e** (22%). ^{1}H NMR (600 MHz, $CDCl_3$) δ 7.54 (s, 2H), 7.32 (m, 10H), 7.14 (s, 2H), 4.29 (s, 4H), 4.02 (s, 6H), 3.96 (s, 6H), 3.49 (s, 6H), 2.02 (s, 6H). To a solution of compound **10e** (170 mg, 0.29 mmol) in 10 mL TFA was added 0.6 mL of triethylsilane dropwise. The solution was stirred overnight at room temperature and concentrated in *vacuo* followed by silica gel column chromatography to give compound **11e** as colorless oil (140 mg, 90%). ^{1}H NMR (600 MHz, $CDCl_3$) δ 7.67 (s, 2H), 7.44 (s, 2H), 7.35 (s, 8H), 7.25 (s, 2H), 4.04 (s, 6H), 3.95 (s, 6H), 3.60 (s, 6H), 3.41 (m, 4H), 3.02 (m, 4H), 2.18 (s, 6H).

3,3′-Dimethyl-5,5′-diphenethyl-2,2′-binaphthyl-1,1′,6,6′,7,7′-hexaol (12e)—0.27 mL of BBr_3 solution (0.72 g, 2.88 mmol) was added dropwise into a solution of **11e** (200 mg, 0.30 mmol) in 8 mL of anhydrous CH_2Cl_2 at −78 °C. Stirring was continued at −78 °C for 1 h, 0 °C for 1 h, and ambient temperature for 1 h, respectively. 100 grams of ice containing 10 mL of 6M HCl was added to the mixture and stirred for 1 h at room temperature. The aqueous layer was extracted with dichloromethane (3 × 50 mL). The combined organic layer was washed with water, brine and dried over $MgSO_4$. The solvent was concentrated *in vacuo* and the residue was purified by C-18 column chromatography (H_2O/Acetonitrile) to give 128 mg of compound **12e** (75%) as orange solid. ^{1}H NMR (600 MHz, $CDCl_3$) δ 7.52 (s, 2H), 7.44 (s, 2H), 7.30 (m, 10H), 5.35 (s, OH, 4H), 5.17 (s, OH, 2H), 3.37 (t, $J_1 = J_2$ = 6.6 Hz, 4H), 3.03 (t, $J_1 = J_2$ = 6.6 Hz, 4H), 2.13 (s, 6H). HPLC purity 99.5%, t_R = 14.93 min. HRMS calcd for $\mathbf{C_{38}H_{34}O_6}$ 587.2428 (M + H), found 587.2425.

Following above mentioned procedure and the appropriate starting materials and reagents used; compounds 12a–12e were synthesized.

5,5′-Diisobutyl-3,3′-dimethyl-2,2′-binaphthyl-1,1′,6,6′,7,7′-hexaol (12a)—Yield, 80%; ^{1}H NMR (600 MHz, CD_3OD) δ 7.44 (s, 2H), 7.34 (s, 2H), 2.95 (d, J = 7.2 Hz, 4H), 2.14 (m, 2H), 2.05 (s, 6H), 1.02 (d, J = 6.0 Hz, 6H), 1.00 (d, J = 6.0 Hz, 6H). HPLC purity 98.5%, t_R = 13.19 min. HRMS calcd for $\mathbf{C_{30}H_{34}O_6}$ 491.2428 (M + H), found 491.2429.

5,5′-Diisopentyl-3,3′-dimethyl-2,2′-binaphthyl-1,1′,6,6′,7,7′-hexaol (12b)—Yield, 79%; ^{1}H NMR (600 MHz, CD_3OD) δ 7.42 (s, 2H), 7.34 (s, 2H), 3.04 (t, $J_1 = J_2$ = 5.4 Hz, 4H), 2.05 (s, 6H), 1.74 (m, 2H), 1.55 (m, 4H), 1.05 (d, J = 3.6 Hz, 6H), 1.04 (d, J = 3.6 Hz, 6H). HPLC purity 99.5%, t_R = 15.56 min. HRMS calcd for $\mathbf{C_{32}H_{38}O_6}$ 519.2741 (M + H), found 519.2739.

5,5′-Bis(cyclopentylmethyl)-3,3′-dimethyl-2,2′-binaphthyl-1,1′,6,6′,7,7′-hexaol (12c)—Yield, 78%; ^{1}H NMR (600 MHz, CD_3OD) δ 7.41 (s, 2H), 7.37 (s, 2H), 3.06 (d, J = 7.2 Hz, 4H), 2.36 (m, 2H), 2.03 (s, 6H), 1.72 (m, 8H), 1.50 (m, 8H). HPLC purity 99.5%, t_R = 16.93 min. HRMS calcd for $\mathbf{C_{34}H_{38}O_6}$ 543.2741 (M + H), found 543.2739.

5,5′-Dibenzyl-3,3′-dimethyl-2,2′-binaphthyl-1,1′,6,6′,7,7′-hexaol (12d)—Yield, 72%; ^{1}H NMR (600 MHz, $(CD_3)_2SO$) δ 9.81 (s, 2H), 8.64 (s, 2H), 7.76 (s, 2H), 7.39 (s, 2H), 7.24 (m, 10H), 7.10 (m, 2H), 4.28 (dd, J_1 = 15.0 Hz, J_2 = 19.8 Hz, 4H), 1.94 (s, 6H). HPLC purity 97.5%, t_R = 10.64 min. HRMS calcd for $\mathbf{C_{36}H_{30}O_6}$ 559.2115 (M + H), found 559.2112.

3,3′-Dimethyl-2,2′-binaphthyl-1,1′,6,6′,7,7′-hexaol (13)—The compound **4** (2.8 g, 5.1 mmol) was added in portions to 36 mL of concentrated sulfuric acid. The solution was vigorous stirring for 50 min at room temperature. The reaction mixture was poured onto ice and water mixture. The solution was extracted with chloroform and the organic layer was washed with

water, dilute ammonium hydroxide, and brine, dried, and concentrated under vacuum. Purification by flash chromatography (10% acetonitrile in CH_2Cl_2) followed by recrystallization from benzene/methanol afforded 1.2 g white solid as methylated compound **13**. 0.27 mL of BBr_3 solution (0.72 g, 2.88 mmol) was added dropwise into a solution of the above white solid (87 mg, 0.19 mmol) in 8 mL of anhydrous CH_2Cl_2 at −78 °C. Stirring was continued at −78 °C for 1 h, 0 °C for 1 h, and ambient temperature for 1 h, respectively. 100 grams of ice containing 10 mL of 6M HCl was added to the mixture and stirred for 1 h at room temperature. The aqueous layer was extracted with dichloromethane (3 × 50 mL). The combined organic layer was washed with water, brine and dried over $MgSO_4$. The solvent was concentrated *in vacuo* and the residue was purified by C-18 column chromatography (H_2O/Acetonitrile) to give 57 mg of compound **13** (80%) as white solid. ^{1}H NMR (600 MHz, CD_3OD) δ 7.46 (s, 2H), 7.11 (s, 2H), 7.02 (s, 2H), 1.97 (s, 6H). HPLC purity 99.0%, t_R = 3.46 min. HRMS calcd for $\mathbf{C_{22}H_{18}O_6}$ 379.1176 (M + H), found 379.1168.

Following above demethylation procedure, compound **14** was synthesized.

1,1′,6,6′,7,7′-Hexahydroxy-3,3′-dimethyl-2,2′-binaphthyl-5,5′-dicarboxylic acid (14)—Yield, 70%; ^{1}H NMR (600 MHz, CD_3OD) δ 8.29 (s, 2H), 7.83 (s, 2H), 2.04 (s, 6H). HPLC purity 99.4%, t_R = 2.56 min. HRMS calcd for $\mathbf{C_{24}H_{18}O_{10}}$ 467.0973 (M + H), found 467.0964.

Molecular Modeling

Molecular modeling studies were conducted on a Linux workstation and a 64 × 3.2-GHz CPUs Linux cluster. Docking studies were performed using the crystal structure of Bcl-2 in complex with a benzothiazole BH3 mimetic ligand (Protein Data Bank code 1YSW).[24, 25] The ligand was extracted from the protein structure and was used to define the binding site for small molecules. Compound **2** and its derivatives were docked into the Bcl-2 protein by the GOLD [39] docking program using ChemScore [40] as the scoring function. The active site radius was set at 10 Å and 10 GA solutions were generated for each molecule. The GA docking procedure in GOLD [39] allowed the small molecules to flexibly explore the best binding conformations whereas the protein structure was kept static. The protein surface was prepared with the program MOLCAD [41] as implemented in Sybyl (Tripos, St. Louis) and was used to analyze the binding poses for the studied small molecules.

Fluorescence Polarization Assays (FPAs)

A Bak BH3 peptide (F-BakBH3) (GQVGRQLAIIGDDINR) was labeled at the N-terminus with fluorescein isothiocyanate (FITC) (Molecular Probes) and purified by HPLC. For competitive binding assays, 100 nM GST–Bcl-X_L ΔTM protein was preincubated with the tested compound at varying concentrations in 47.5 μL PBS (pH=7.4) in 96-well black plates at room temperature for 10 min, then 2.5 μL of 100 nM FITC-labeled Bak BH3 peptide was added to produce a final volume of 50 μL. The wild-type and mutant Bak BH3 peptides were included in each assay plate as positive and negative controls, respectively. After 30 min incubation at room temperature, the polarization values in millipolarization units [42] were measured at excitation/emission wavelengths of 480/535 nm with a multilabel plate reader (PerkinElmer). IC_{50} was determined by fitting the experimental data to a sigmoidal dose-response nonlinear regression model (SigmaPlot 10.0.1, Systat Software, Inc., San Jose, CA, USA). Data reported are mean of three independent experiments ± standard error (SE). Performance of Bcl-2 and Mcl-1 FPA are similar. Briefly, 50 nM of GST-Bcl-2 or -Mcl-1 were incubated with various concentrations of compound **2**, or its 5, 5′ substituted derivatives for 2 min, then 15 nM FITC-conjugated-Bim BH3 peptide [43] was added in PBS buffer. Fluorescence polarization was measured after 10 min.

Cell Viability and Apoptosis Assays

The activity of the compounds against human cancer cell lines (PC3ML, H460, H1299, RS11846) was assessed by using the ATP-LITE assay (PerkinElmer). All cells were seeded in either 12F2 or RPMI1640 medium with 5 mM L-glutamine supplemented with 5% fetal bovine serum (Mediatech Inc.), penicillin and streptomycin (Omega). For maintenance, cells were cultured in 5% FBS. Cells plated into 96 well plates at varying initial densities depending on doubling time. H460 and H1299 plated at 2000 cells/well, A549 and PC3 at 3000 cells/well, and RS118456S at 10,000 cells/well. Compounds were diluted to final concentrations with 0.1% DMSO. Prior to dispensing compounds onto cells, fresh 5% media was placed into wells. Administration of compounds occurred 24 hours after seeding into the fresh media. Cell viability was evaluated using ATP-LITE reagent (PerkinElmer) after 72 hours of treatment. Data were normalized to the DMSO control-treated cells using Prism version 5.01 (Graphpad Software).

The apoptotic activity of the compounds against RS11846 cells was assessed by staining with Annexin V- and propidium iodide (PI). Lymphoma cell line, RS11846, was cultured in RPMI 1640 medium (Mediatech Inc., Herndon, VA 20171) containing 10% fetal bovine serum (Mediatech Inc., Herndon, VA 20171) and Penicillin/Streptomycin (Mediatech Inc., Herndon, VA 20171). Cells were cultured with various concentrations of 5, 5′ substituted compound **2** derivatives for 1 – 2 days. The percentage of viable cells was determined by FITC-Annexin V- and propidium iodide (PI)-labeling, using an Apoptosis Detection kit (BioVision Inc.), and analyzing stained cells by flow cytometry (FACSort; Bectin-Dickinson, Inc.; Mountain View, CA). Cells that were annexin-V-negative and PI-negative were considered viable.

The apoptotic activity of the compounds, such as **8r** and **8q** against mouse embryonic fibroblast wild-type cells (wt-MEFs) and mouse embryonic fibroblast BAX/Bak double knockout cells (DKO/MEFs) was assessed by staining with Annexin V- and propidium iodide (PI). Wild-type MEFs and DKO/MEFs were seeded in 24-well plate at a seeding density of half a million per well (in 1 ml of DMEM medium supplemented by 10% FCS). Next day, compound was added to wild-type and DKO cells at final concentration of 0, 2.5, 5.0, 7.5 and 10 μM. On the following day, floating cells were pooled with adherent cells harvested after brief incubation with 0.25% Trypsin/EDTA solution (Gibco/In-Vitrogen Inc.). Cells were centrifuged and supernatant was discarded, and cell pellet was re-suspended with 0.2 ml of Annexin-V binding buffer, followed by addition of 1 μl Annexin-FITC and 1 μl PI (propidium iodide). The percentage of viable cells was determined by a 3-color FACSort instrument and data analyzed by Flow-Jo program, scoring Annexin V-negative, PI-negative as viable cells.

Bcl-2 Transgenic Mice Studies

Transgenic mice expressing Bcl-2 have been previously described.[44] The *BCL-2* transgene represents a minigene version of a t(14;18) translocation in which the human *BCL-2* gene is fused with the immunoglobulin heavy-chain (IgH) locus and associated IgH enhancer. The transgene was propagated on the Balb/c background. These mice develop polyclonal B-cell hyperplasia with asynchronous transformation to monoclonal aggressive lymphomas beginning at approximately 6 months of age, with approximately 90% of mice undergoing transformation by the age of 12 to 24 months. All animals used here had not yet developed aggressive lymphoma.

Mouse Experiments

Compounds dissolved in 500 μL of solution (Ethanol: Cremophor EL: Saline = 10: 10: 80) were injected intraperitoneally to age- and sex-matched B6Bcl2 mouse, while control-mice were injected intraperitoneally with 500 μL of the same formulation without compound. After 24 hours, B6Bcl2 mice were sacrificed by intraperitoneal injection of lethal dose of Avertin.

Spleen was removed and weighed. The spleen weight of mice is used as an end-point for assessing activity as we determined that spleen weight is highly consistent in age- and sex-matched Bcl-2-transgenic mice in preliminary studies.[20] Variability of spleen weight was within ±2% among control-treated age-matched, sex-matched B6Bcl2 mice.

Supplementary Material

Refer to Web version on PubMed Central for supplementary material.

Acknowledgments

We thank NIH (Grant CA113318 to MP and JCR) and Coronado Biosciences (CSRA #08-02) for financial support.

Abbreviations list

Bcl-2
B-cell lymphoma/leukemia-2

EDCI
1-ethyl-3-(3′-dimethylaminopropyl)carbodiimide

1D-^{1}H NMR
one-dimensional ^{1}H nuclear magnetic resonance spectroscopy

SAR
Structure-activity relationship

FPA
Fluorescence Polarization Assays

ITC
Isothermal Titration Calorimetry

WT
Wild type

MEFs
Mouse embryonic fibroblast cells

DKO
Bax/Bak Double knockout

DKO/MEFs
Bax/Bak Double knockout mouse embryonic fibroblast cells

ACN
Acetonitrile

LC-MS
Liquid chromatography and tandem mass spectrometry

HPLC
High-performance liquid chromatography

TROSY
Transverse Relaxation-Optimized Spectroscopy

ADME

Absorption, Distribution, Metabolism, and Excretion

DMSO
Dimethyl sulphoxide

PAMPA
Parallel artificial membrane permeation assay

FITC
Fluorescein isothiocyanate

GST
Glutathione-S-transferase

PBS
Phosphate-buffered saline

SE
Standard error

PI
Propidium iodide

NADPH
Nicotinamide adenine dinucleotide phosphate

Rpm
Rotations Per Minute

AUC
Area under the curve

References

1. Vaux DL, Korsmeyer SJ. Cell death in development. Cell 1999;96:245–254. [PubMed: 9988219]
2. Reed JC. Dysregulation of apoptosis in cancer. J Clin Oncol 1999;17:2941–2953. [PubMed: 10561374]
3. Johnstone RW, Ruefli AA, Lowe SW. Apoptosis: a link between cancer genetics and chemotherapy. Cell 2002;108:153–164. [PubMed: 11832206]
4. Reed JC. Apoptosis-based therapies. Nature reviews Drug discovery 2002;1:111–121.
5. Reed JC. Molecular biology of chronic lymphocytic leukemia: implications for therapy. Seminars in hematology 1998;35:3–13. [PubMed: 9685174]
6. Adams JM, Cory S. The Bcl-2 protein family: arbiters of cell survival. Science (New York, N Y) 1998;281:1322–1326.
7. Gross A, McDonnell JM, Korsmeyer SJ. BCL-2 family members and the mitochondria in apoptosis. Genes & development 1999;13:1899–1911. [PubMed: 10444588]
8. Wang JL, Liu D, Zhang ZJ, Shan S, Han X, Srinivasula SM, Croce CM, Alnemri ES, Huang Z. Structure-based discovery of an organic compound that binds Bcl-2 protein and induces apoptosis of tumor cells. Proceedings of the National Academy of Sciences of the United States of America 2000;97:7124–7129. [PubMed: 10860979]
9. Degterev A, Lugovskoy A, Cardone M, Mulley B, Wagner G, Mitchison T, Yuan J. Identification of small-molecule inhibitors of interaction between the BH3 domain and Bcl-xL. Nat Cell Biol 2001;3:173–182. [PubMed: 11175750]
10. Reed JC. Bcl-2 family proteins. Oncogene 1998;17:3225–3236. [PubMed: 9916985]
11. Reed JC. Bcl-2 family proteins: strategies for overcoming chemoresistance in cancer. Advances in pharmacology (San Diego, Calif) 1997;41:501–532.

12. Kitada S, Leone M, Sareth S, Zhai D, Reed JC, Pellecchia M. Discovery, characterization, and structure-activity relationships studies of proapoptotic polyphenols targeting B-cell lymphocyte/leukemia-2 proteins. Journal of medicinal chemistry 2003;46:4259–4264. [PubMed: 13678404]

13. Zhang M, Liu H, Guo R, Ling Y, Wu X, Li B, Roller PP, Wang S, Yang D. Molecular mechanism of gossypol-induced cell growth inhibition and cell death of HT-29 human colon carcinoma cells. Biochemical pharmacology 2003;66:93–103. [PubMed: 12818369]

14. Wang G, Nikolovska-Coleska Z, Yang CY, Wang R, Tang G, Guo J, Shangary S, Qiu S, Gao W, Yang D, Meagher J, Stuckey J, Krajewski K, Jiang S, Roller PP, Abaan HO, Tomita Y, Wang S. Structure-based design of potent small-molecule inhibitors of anti-apoptotic Bcl-2 proteins. Journal of medicinal chemistry 2006;49:6139–6142. [PubMed: 17034116]

15. Oliver CL, Miranda MB, Shangary S, Land S, Wang S, Johnson DE. (−)-Gossypol acts directly on the mitochondria to overcome Bcl-2- and Bcl-X(L)-mediated apoptosis resistance. Mol Cancer Ther 2005;4:23–31. [PubMed: 15657350]

16. Mohammad RM, Wang S, Aboukameel A, Chen B, Wu X, Chen J, Al-Katib A. Preclinical studies of a nonpeptidic small-molecule inhibitor of Bcl-2 and Bcl-X(L) [(−)-gossypol] against diffuse large cell lymphoma. Mol Cancer Ther 2005;4:13–21. [PubMed: 15657349]

17. Wang, S.; Yang, D. Small Molecular Antagonists of Bcl-2 family proteins. May 30. 2002 US patent applications series no. 2003008924

18. Meng Y, Tang W, Dai Y, Wu X, Liu M, Ji Q, Ji M, Pienta K, Lawrence T, Xu L. Natural BH3 mimetic (−)-gossypol chemosensitizes human prostate cancer via Bcl-xL inhibition accompanied by increase of Puma and Noxa. Mol Cancer Ther 2008;7:2192–2202. [PubMed: 18645028]

19. Becattini B, Kitada S, Leone M, Monosov E, Chandler S, Zhai D, Kipps TJ, Reed JC, Pellecchia M. Rational design and real time, in-cell detection of the proapoptotic activity of a novel compound targeting Bcl-X(L). Chemistry & biology 2004;11:389–395. [PubMed: 15123268]

20. Kitada S, Kress CL, Krajewska M, Jia L, Pellecchia M, Reed JC. Bcl-2 antagonist apogossypol (NSC736630) displays single-agent activity in Bcl-2-transgenic mice and has superior efficacy with less toxicity compared with gossypol (NSC19048). Blood 2008;111:3211–3219. [PubMed: 18202226]

21. Coward L, Gorman G, Noker P, Kerstner-Wood C, Pellecchia M, Reed JC, Jia L. Quantitative determination of apogossypol, a pro-apoptotic analog of gossypol, in mouse plasma using LC/MS/MS. Journal of pharmaceutical and biomedical analysis 2006;42:581–586. [PubMed: 16859853]

22. Wei J, Rega MF, Kitada S, Yuan H, Zhai D, Risbood P, Seltzman HH, Twine CE, Reed JC, Pellecchia M. Synthesis and evaluation of Apogossypol atropisomers as potential Bcl-xL antagonists. Cancer Lett 2009;273:107–113. [PubMed: 18782651]

23. Jun Wei SK, Rega Michele F, Emdadi Aras, Yuan Hongbin, Cellitti Jason, Stebbins John L, Zhai Dayong, Sun Jiazhi, Yang Li, Dahl Russell, Zhang Ziming, Wu Bainan, Wang Si, Reed Tyler A, Lawrence Nicholas, Sebti Said, Pellecchia JCRaM. Apogossypol Derivatives as Antagonists of Anti-apoptotic Bcl-2 Family Proteins. Mol Cancer Ther 2009;8:904–913. [PubMed: 19372563]

24. Oltersdorf T, Elmore SW, Shoemaker AR, Armstrong RC, Augeri DJ, Belli BA, Bruncko M, Deckwerth TL, Dinges J, Hajduk PJ, Joseph MK, Kitada S, Korsmeyer SJ, Kunzer AR, Letai A, Li C, Mitten MJ, Nettesheim DG, Ng S, Nimmer PM, O'Connor JM, Oleksijew A, Petros AM, Reed JC, Shen W, Tahir SK, Thompson CB, Tomaselli KJ, Wang B, Wendt MD, Zhang H, Fesik SW, Rosenberg SH. An inhibitor of Bcl-2 family proteins induces regression of solid tumours. Nature 2005;435:677–681. [PubMed: 15902208]

25. Bruncko M, Oost TK, Belli BA, Ding H, Joseph MK, Kunzer A, Martineau D, McClellan WJ, Mitten M, Ng SC, Nimmer PM, Oltersdorf T, Park CM, Petros AM, Shoemaker AR, Song X, Wang X, Wendt MD, Zhang H, Fesik SW, Rosenberg SH, Elmore SW. Studies leading to potent, dual inhibitors of Bcl-2 and Bcl-xL. J Med Chem 2007;50:641–662. [PubMed: 17256834]

26. Meltzer PC, Bickford HP, Lambert GJ. A Regioselective Route to Gossypol Analogues: The Synthesis of Gossypol and 5,5′-Didesisopropyl-5,5′-diethylgossypol. J Org Chem 1985;50:3121–3124.

27. Royer RE, Deck LM, Vander Jagt TJ, Martinez FJ, Mills RG, Young SA, Vander Jagt DL. Synthesis and anti-HIV activity of 1,1′-dideoxygossypol and related compounds. J Med Chem 1995;38:2427–2432. [PubMed: 7608907]

28. Yamanoi Y, Nishihara H. Direct and selective arylation of tertiary silanes with rhodium catalyst. J Org Chem 2008;73:6671–6678. [PubMed: 18681401]
29. Tang G, Ding K, Nikolovska-Coleska Z, Yang CY, Qiu S, Shangary S, Wang R, Guo J, Gao W, Meagher J, Stuckey J, Krajewski K, Jiang S, Roller PP, Wang S. Structure-based design of flavonoid compounds as a new class of small-molecule inhibitors of the anti-apoptotic Bcl-2 proteins. J Med Chem 2007;50:3163–3166. [PubMed: 17552510]
30. Rega MF, Leone M, Jung D, Cotton NJ, Stebbins JL, Pellecchia M. Structure-based discovery of a new class of Bcl-xL antagonists. Bioorg Chem 2007;35:344–353. [PubMed: 17512966]
31. Wesarg E, Hoffarth S, Wiewrodt R, Kroll M, Biesterfeld S, Huber C, Schuler M. Targeting BCL-2 family proteins to overcome drug resistance in non-small cell lung cancer. Int J Cancer 2007;121:2387–2394. [PubMed: 17688235]
32. Brien G, Trescol-Biemont MC, Bonnefoy-Berard N. Downregulation of Bfl-1 protein expression sensitizes malignant B cells to apoptosis. Oncogene 2007;26:5828–5832. [PubMed: 17353899]
33. Li J, Viallet J, Haura EB. A small molecule pan-Bcl-2 family inhibitor, GX15-070, induces apoptosis and enhances cisplatin-induced apoptosis in non-small cell lung cancer cells. Cancer Chemother Pharmacol 2008;61:525–534. [PubMed: 17505826]
34. Voortman J, Checinska A, Giaccone G, Rodriguez JA, Kruyt FA. Bortezomib, but not cisplatin, induces mitochondria-dependent apoptosis accompanied by up-regulation of noxa in the non-small cell lung cancer cell line NCI-H460. Mol Cancer Ther 2007;6:1046–1053. [PubMed: 17363497]
35. Ferreira CG, Span SW, Peters GJ, Kruyt FA, Giaccone G. Chemotherapy triggers apoptosis in a caspase-8-dependent and mitochondria-controlled manner in the non-small cell lung cancer cell line NCI-H460. Cancer Res 2000;60:7133–7141. [PubMed: 11156422]
36. Cory S, Adams JM. Killing cancer cells by flipping the Bcl-2/Bax switch. Cancer cell 2005;8:5–6. [PubMed: 16023593]
37. Wei MC, Zong WX, Cheng EH, Lindsten T, Panoutsakopoulou V, Ross AJ, Roth KA, MacGregor GR, Thompson CB, Korsmeyer SJ. Proapoptotic BAX and BAK: a requisite gateway to mitochondrial dysfunction and death. Science (New York, N Y) 2001;292:727–730.
38. Vogler M, Weber K, Dinsdale D, Schmitz I, Schulze-Osthoff K, Dyer MJ, Cohen GM. Different forms of cell death induced by putative Bcl2 inhibitors. Cell Death and Differentiation 2009:1–10. [PubMed: 19079285]
39. Jones G, Willett P, Glen RC, Leach AR, Taylor R. Development and validation of a genetic algorithm for flexible docking. Journal of molecular biology 1997;267:727–748. [PubMed: 9126849]
40. Eldridge MD, Murray CW, Auton TR, Paolini GV, Mee RP. Empirical scoring functions: I. The development of a fast empirical scoring function to estimate the binding affinity of ligands in receptor complexes. J Comput Aided Mol Des 1997;11:425–445. [PubMed: 9385547]
41. Teschner M, Henn C, Vollhardt H, Reiling S, Brickmann J. Texture mapping: a new tool for molecular graphics. J Mol Graph 1994;12:98–105. [PubMed: 7918258]
42. Sattler M, Liang H, Nettesheim D, Meadows RP, Harlan JE, Eberstadt M, Yoon HS, Shuker SB, Chang BS, Minn AJ, Thompson CB, Fesik SW. Structure of Bcl-xL-Bak peptide complex: recognition between regulators of apoptosis. Science (New York, N Y) 1997;275:983–986.
43. Ramjaun AR, Tomlinson S, Eddaoudi A, Downward J. Upregulation of two BH3-only proteins, Bmf and Bim, during TGF beta-induced apoptosis. Oncogene 2007;26:970–981. [PubMed: 16909112]
44. Katsumata M, Siegel RM, Louie DC, Miyashita T, Tsujimoto Y, Nowell PC, Greene MI, Reed JC. Differential effects of Bcl-2 on T and B cells in transgenic mice. Proc Natl Acad Sci U S A 1992;89:11376–11380. [PubMed: 1454823]

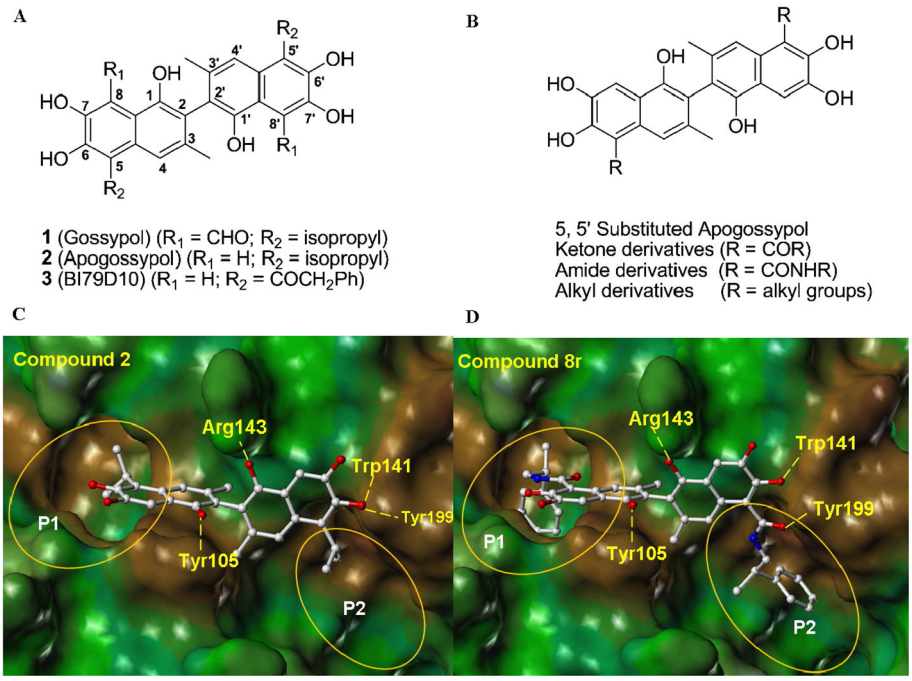

Figure 1.

(A) Structure of compound **1, 2** and **3. (B)** Structure of 5, 5′ substituted compound **2** derivatives. **(C)** and **(D),** Molecular docking studies. Stereo views of docked structures of **(C)** compound **2** and **(D)** compound **8r** into Bcl-2 (PDB ID:1YSW).

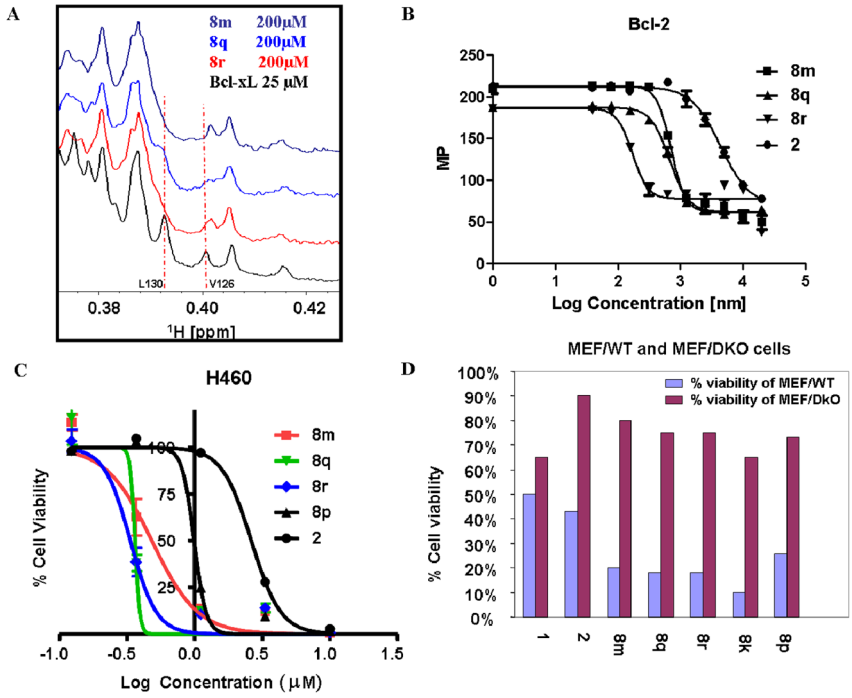

Figure 2.

(A) NMR binding studies. Aliphatic region of the ^{1}H-NMR spectrum of Bcl-X_L (25 μM, black) and Bcl-X_L in the presence of compound **8m** (200 μM, grey), **8q** (200 μM, blue), and **8r** (200 μM, red). **(B)** Fluorescence polarization-based competitive binding curves of compound **8m** (solid squares), **8q** (solid up triangle), **8r** (solid down triangle) and **2** (solid dots) using Bcl-2. **(C)** Inhibition of cell growth by compound **8m** (red square), **8q** (green triangle), **8r** (blue diamond), **8p** (dark triangle) and **2** (dark dots) in the H460 human lung cell line. Cells were treated for 3 days and cell viability was evaluated using ATP-LITE assay. **(D)** Mouse embryonic fibroblast cells with wild-type (MEF/WT; blue bars) or *bax*$^{-/-}$*bak*$^{-/-}$ double knockout (red bars) genotypes were treated with various 5, 5′ substituted compound **2** derivatives at 10 μM and apoptosis was monitored by Annexin V-FITC assays.

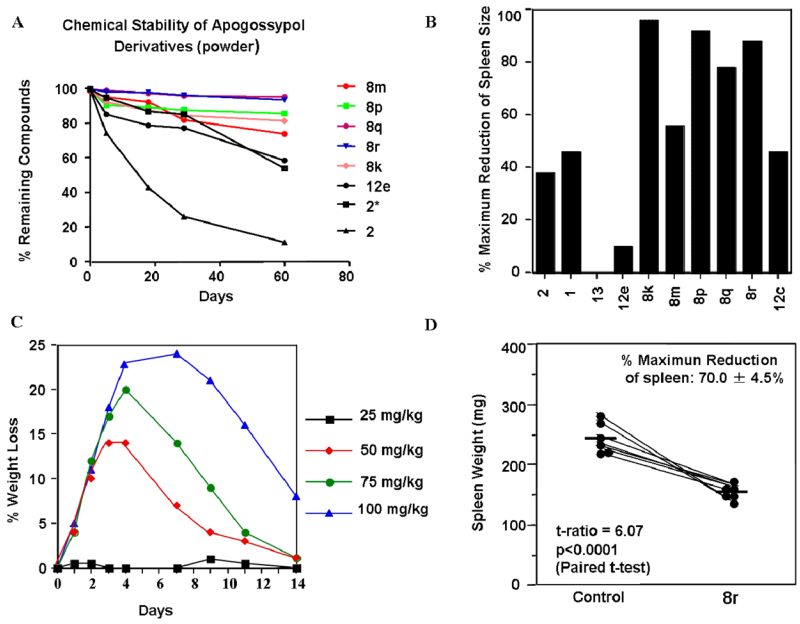

Figure 3.

Characterization of compounds *in vitro* and *in vivo*. **(A)** Chemical stability of 5, 5′-substituted compound **2** derivatives when left at room temperature in powder form: **8m** (red dot), **8p** (green square), **8q** (purple dot), **8r** (blue triangle), **8k** (pink dot), **12e** (dark dot), **2*** (compound **2** with ascorbic acid, dark square) and **2** (pure **2**, dark triangle). Chemical stability was evaluated in the air for 60 days at room temperature. The stability was monitored using a combination of HPLC and LCMS. **(B)** Effects of 5, 5′ substituted compound **2** derivatives on shrinkage of Bcl-2 mouse spleen at a single intraperitoneal injection dose of 0.072 mmol/kg. All shrinkage data are percentage of maximum reduction of mice spleen size. **(C)** % Weight loss in mice induced by single ip injection of various amount of compound **8r. (D)** Effects of compound **8r** at 42 mg/kg (0.06 mmol/kg) on reduction of spleen weight of six Bcl-2 mice treatment with a single intraperitoneal injection. Data shown as means ± S.E. (n =6). $P < 0.0001$.

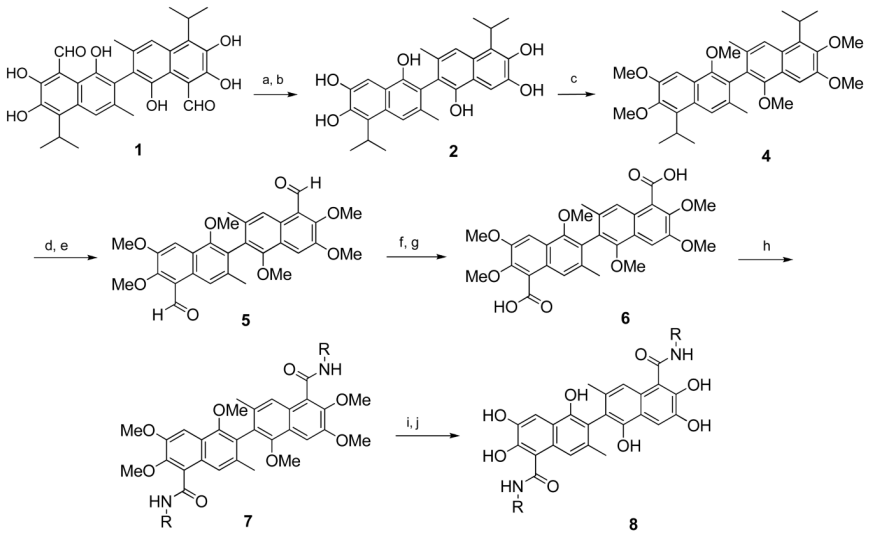

Scheme 1.

Reagents and conditions: (a) NaOH, H_2O, reflux; (b) H_2SO_4; (c) DMS, K_2CO_3; (d) $TiCl_4$, Cl_2CHOCH_3, rt; (e) HCl, H_2O (f) $NaClO_2$, H_2O_2, KH_2PO_4, CH_3CN, rt; (g) HCl, H_2O; (h) EDCI, NH_2R, HOBT, rt; (i) BBr_3, CH_2Cl_2 (j) HCl, H_2O.

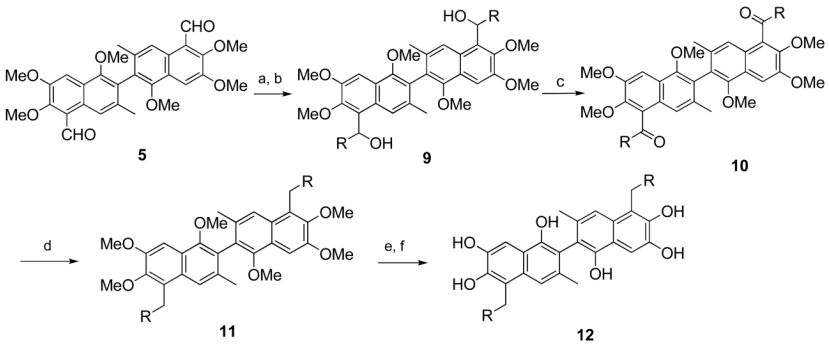

Scheme 2.

Reagents and conditions: (a) RMgBr or RLi, rt; (b) NH_4Cl, H_2O; (c) Pyridinium chlorochromate, CH_2Cl_2, rt; (d) Et_3SiH, TFA or Pd/C, H_2; (e) BBr_3; (f) HCl, H_2O.

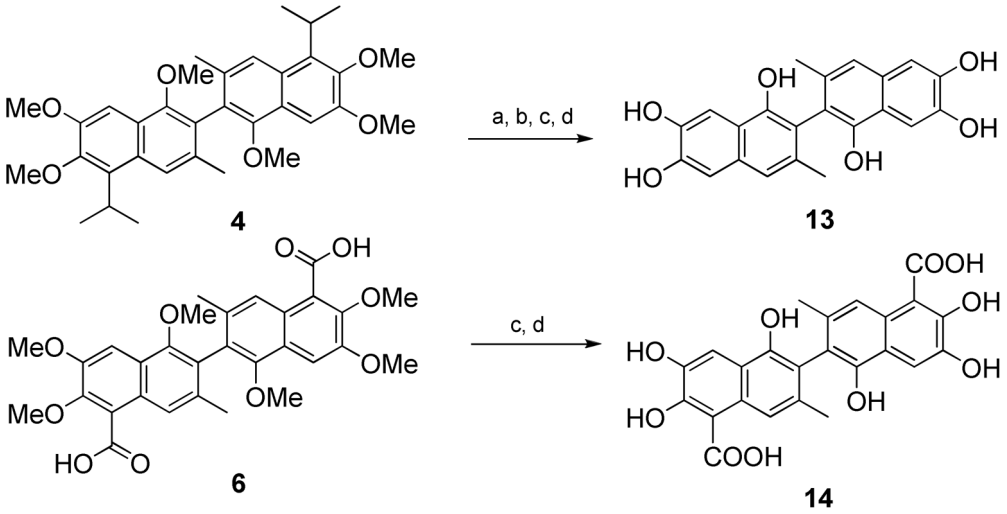

Scheme 3.

Reagents and conditions: (a) H_2SO_4, rt; (b) H_2O; (c) BBr_3, CH_2Cl_2; (d) HCl, H_2O.

Table 1

Evaluation of 5, 5′ substituted compound 2 derivatives using a combination of 1D ^{1}H-NMR binding assays and cell viability assays

Compound	R =	1D-^{1}H NMR[a*]	EC_{50} (μM) RS11846[c*]	H1299[b*]	H460[b*]	PC3ML[b*]	BP3[c*]
		+++	4.2	6.0	3.0	3.1	1.42

J Med Chem. Author manuscript; available in PMC 2010 July 23.

Compound	R =	1D-^{1}H NMR[a]*	EC_{50} (μM) RS11846[c]*	H1299[b]*	H460[b]*	PC3ML[b]*	BP3[c]*
		++	5.0	3.4	3.5	10.4	4.7

nd	R =	1D-^{1}H NMR[a*]	EC_{50} (μM) RS11846[c*]	H1299[b*]	H460[b*]	PC3ML[b*]	BP3[c*]
	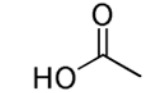	−	>30	>30	>30	>30	>30
	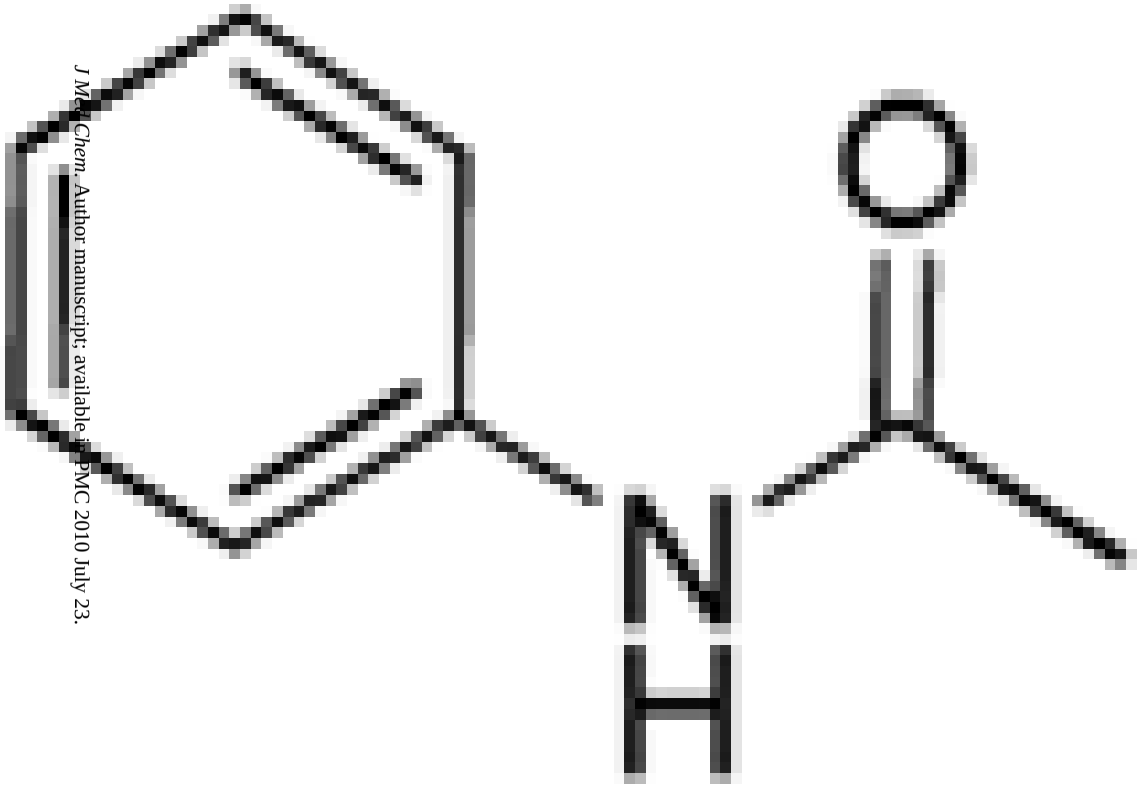	+	15.1	8.0	3.5	15.1	ND[d*]
	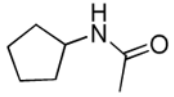	+	13.7	8.0	8.5	12.2	ND

Compound	R =	1D-^{1}H NMR[a]*	EC_{50} (μM) RS11846[c]*	H1299[b]*	H460[b]*	PC3ML[b]*	BP3[c]*
		+	10.8	17.0	10.1	8.5	ND
		+	4.7	5.0	4.1	8.3	ND
		+	12.6	28.7	16.7	12.2	ND
		+++	4.2	ND	1.5	ND	ND

Compound	R =	1D-^{1}H NMR[a]*	EC_{50} (μM)				
			RS11846[c]*	H1299[b]*	H460[b]*	PC3ML[b]*	BP3[c]*
		+	9.3	3.6	4.6	13.7	ND

Compound	R =	1D-^{1}H NMR[a]*	EC_{50} (μM) RS11846[c]*	H1299[b]*	H460[b]*	PC3ML[b]*	BP3[c]*
		+++	4.8	3.1	2.9	10.2	ND

Compound	R =	1D-^{1}H NMR[a]*	EC_{50} (μM) RS11846[c]*	H1299[b]*	H460[b]*	PC3ML[b]*	BP3[c]*
		+++	7.3	5.2	3.3	8.3	ND

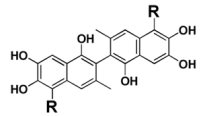

nd	R =	1D-^{1}H NMR[a*]	EC$_{50}$ (μM) RS11846[c*]	H1299[b*]	H460[b*]	PC3ML[b*]	BP3[c*]
	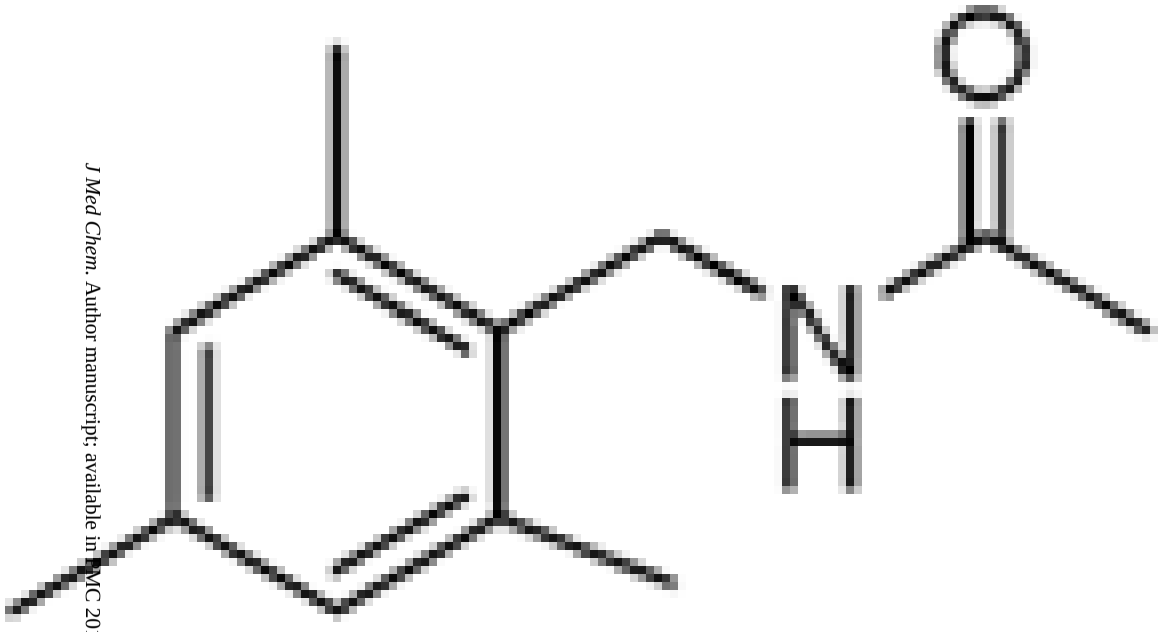	++	3.0	3.6	1.4	0.7	1.5
	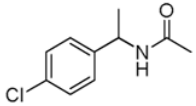	+++	5.5	3.2	0.50	5.0	1.5
	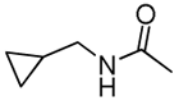	+	>10	ND	ND	ND	ND
	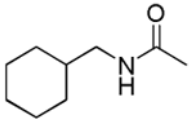	+++	4.9	4.8	0.41	3.7	0.90

J Med Chem. Author manuscript; available in PMC 2010 July 23.

Compound	R =	1D-^{1}H NMR[a]*	EC_{50} (μM)				
			RS11846[c]*	H1299[b]*	H460[b]*	PC3ML[b]*	BP3[c]*
		++	3.1	3.6	0.55	3.9	0.72

Compound	R =	1D-^{1}H NMR[a]*	EC_{50} (μM) RS11846[c]*	H1299[b]*	H460[b]*	PC3ML[b]*	BP3[c]*
		+	5.6	ND	0.70	ND	ND
		+++	4.6	7.8	0.99	3.2	0.41

Compound	R =	1D-^{1}H NMR[a]*	EC_{50} (μM)				
			RS11846[c]*	H1299[b]*	H460[b]*	PC3ML[b]*	BP3[c]*
		+++	3.0	0.36	0.40	1.7	0.2
		++	5.8	3.2	0.33	1.7	0.66

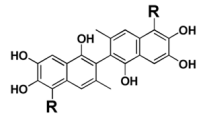

nd	R =	1D-^{1}H NMR[a*]	EC_{50} (μM) RS11846[c*]	H1299[b*]	H460[b*]	PC3ML[b*]	BP3[c*]
	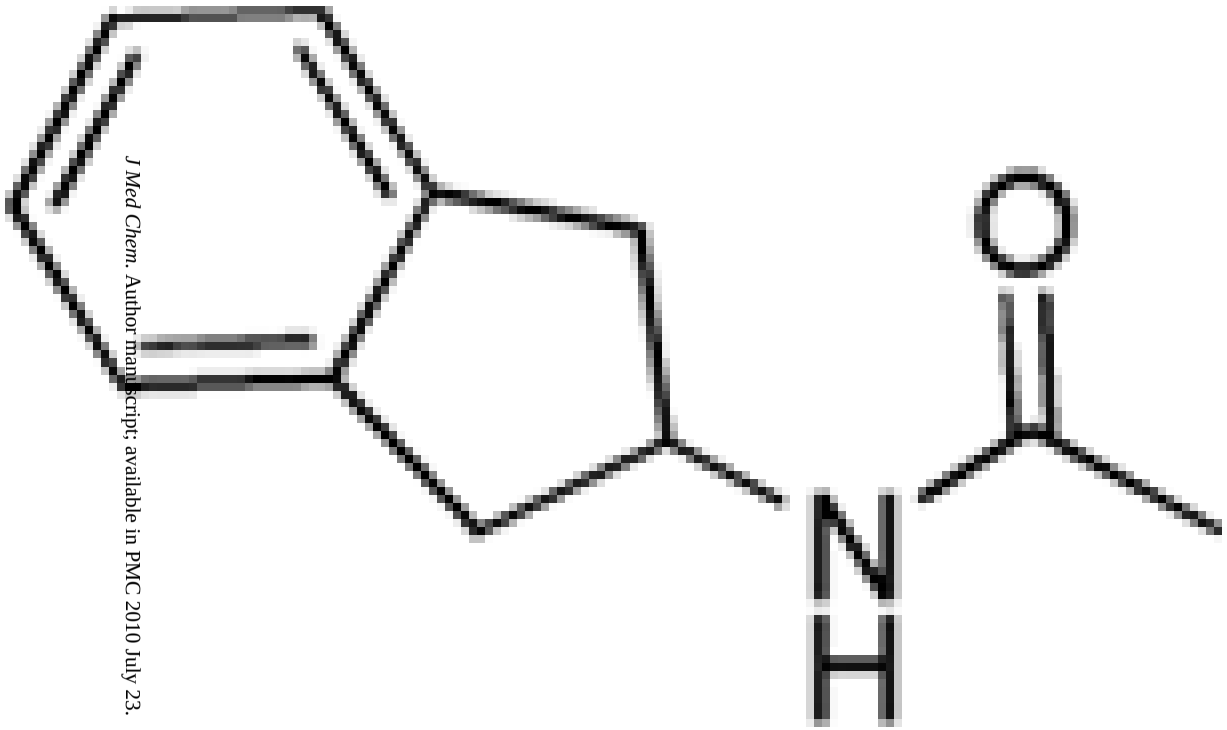	++	4.1	7.1	0.94	3.0	1.1
	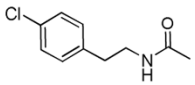	++	5.1	ND	1.3	ND	0.70

-point-rating scale: +++, Very Active; ++, Active; +, Mild; −, Weak

Compounds against cell line using ATP-LITE assay

ompounds against cell line using Annexin V-FITC and propidium iodide assay

ID: not determined

Table 2

Evaluation of 5, 5′ substituted compound 2 derivatives using a combination of 1D ^{1}H-NMR binding assays and cell viability assays

	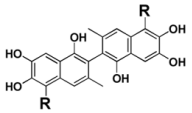		EC_{50} (μM)				
nd	**R =**	**1D-^{1}H NMR[a*]**	**RS11846[c*]**	**H1299[b*]**	**H460[b*]**	**PC3ML[b*]**	**BP3[c*]**
	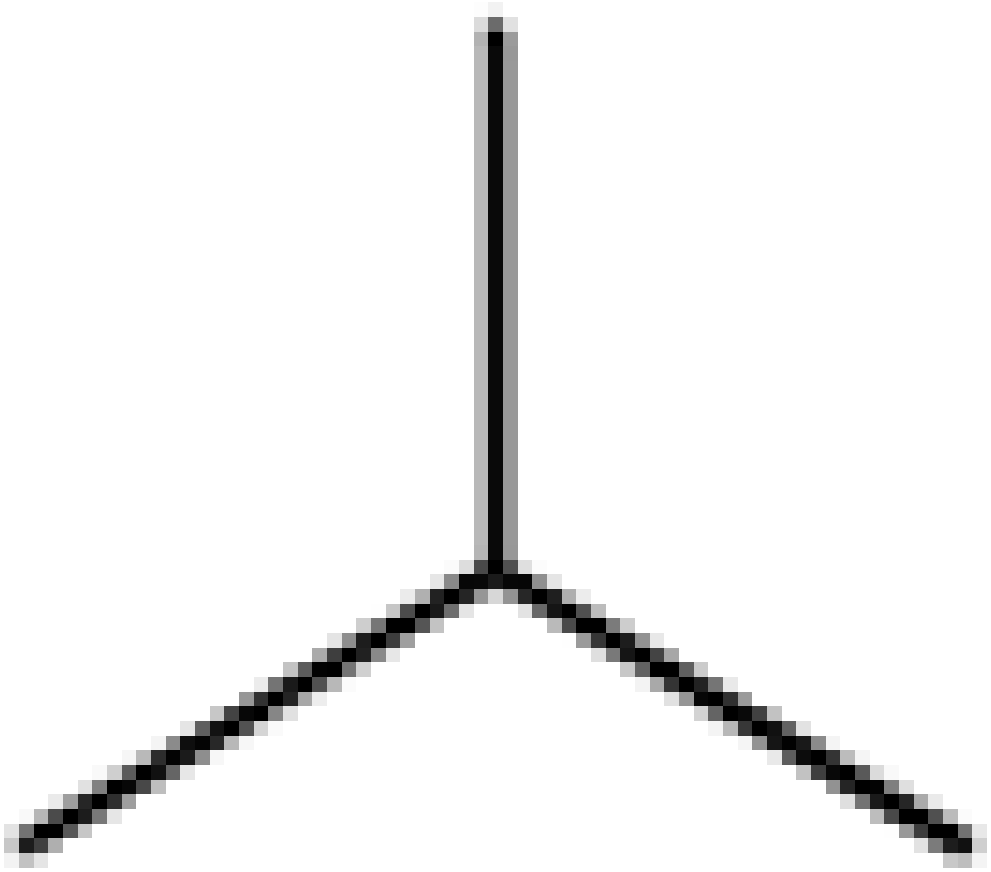	++	5.0	3.4	3.5	10.4	4.7
	H	−	24.5	13.4	>10	>10	ND[D*]

Compound	R =	1D-^{1}H NMR[a]*	EC_{50} (μM) RS11846[c]*	H1299[b]*	H460[b]*	PC3ML[b]*	BP3[c]*
		+	8.4	1.2	3.2	6.7	ND

Compound	R =	1D-^{1}H NMR[a]*	EC_{50} (μM)				
			RS11846[c]*	H1299[b]*	H460[b]*	PC3ML[b]*	BP3[c]*
		+	4.8	1.8	1.1	5.2	ND

Compound	R =	1D-^{1}H NMR[a]*	EC_{50} (μM)				
			RS11846[c]*	H1299[b]*	H460[b]*	PC3ML[b]*	BP3[c]*
		+	4.5	10.9	1.8	11.2	ND

Compound	R =	1D-^{1}H NMR[a]*	EC_{50} (μM) RS11846[c]*	H1299[b]*	H460[b]*	PC3ML[b]*	BP3[c]*
1		+	3.2	1.28	1.2	8.3	ND

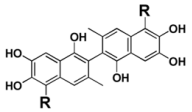

nd	R =	1D-^{1}H NMR[a*]	EC_{50} (μM) RS11846[c*]	H1299[b*]	H460[b*]	PC3ML[b*]	BP3[c*]
	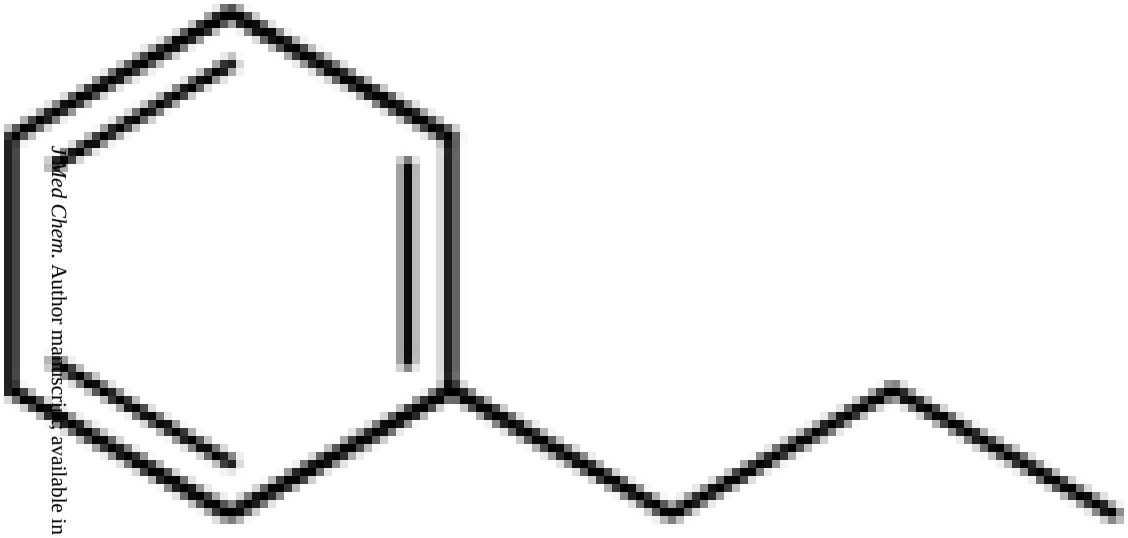	++	9.8	0.58	0.92	2.4	4.14

-point-rating scale: +++: Very Active; ++: Active; +: Mild; −: Weak

Compounds against cell line using ATP-LITE assay

Compounds against cell line using Annexin V-FITC and propidium iodide assay

ND: not determined

Table 3

Cross-activity of selected 5, 5′ substituted compound 2 derivatives against Bcl-X_L, Bcl-2, Mcl-1 and Bfl-1.

Compound	IC_{50} (μM) FPA				K_d (μM) ITC
IC_{50}	Bcl-X_L	Bcl-2	Mcl-1	Bfl-1	Bcl-X_L
2	3.7	4.3	2.6	>10	1.7
12e	3.5	0.48	0.83	5.0	0.41
8m	1.1	0.71	0.78	2.0	0.85
8n	0.80	0.15	0.30	0.55	ND
8p	6.3	4.4	3.2	ND[a*]	ND
8q	0.93	0.67	0.59	1.3	0.12
8j	0.8	0.70	1.1	ND	ND
8k	0.27	0.49	0.23	0.40	0.11
8r	0.76	0.32	0.28	0.73	0.11
8s	0.85	0.70	0.35	0.67	ND

[a*] ND = Not determined

Table 4

Plasma stability, microsomal stability, and cell permeability of selected 5, 5′ substituted compound 2 derivatives.

Compound	Plasma stability (T = 1 h)	Microsomal Stability (T = 1 h)	Cell Permeability
2	53%	64%	−7.16
12e	80%	89%	−6.61
12c	81%	75%	−6.27
8n	63%	60%	−6.49
8m	89%	90%	−6.67
8p	ND[a*]	90%	−7.71
8q	94%	87%	−8.15
8r	96%	76%	−7.51
8k	94%	71%	−7.92

[a*] ND = Not determined